Biosensing Team Twente 2025

Wearable Biosensor for Acute Kidney Injury (AKI)

University of Twente — August 8, 2025

Team Members

Timur Djalilov
Queralt Piferrer Grau
Sarah Foo
Jan Sampol Ramírez
Marc Centelles Molina
Vicent Roig Roig
Aakriti Dawadi
Matteo Pozzato
Andrea D'Silva
Fernando Rodríguez
Paulo Palomo
Sreya Bavoju
Deikshi Kumari

Board

Chair / Secretary — Diana Andreoli
Treasurer / Technical Manager — Jan Pieter de Rie
External Relations Manager — Danail Tsanov
Internal Relations Manager — Vinaya Tennakoon
Communication Manager — Caterina Cattabriga

Supervisors

Dr. Ir. Pep Canyelles Pericas	Bussiness case advisor, Supervisory Board
Dr. Mohammad Saghafi	Chip design, Supervisory Board
Dr. Jannis Schlicke	Laboratory Supervisor
Eng. Amarna Pels	Laboratory Supervisor
Eng. Hanna Reijneveld	Laboratory Supervisor

SensUs

Contents

Abstract

Kidney disease is a growing global health concern, with acute kidney injury (AKI) posing a significant risk due to its rapid onset and potential for irreversible damage. Current diagnostics rely on intermittent blood testing, which cannot capture rapid fluctuations in kidney function. This work presents the development of a wearable biosensor for continuous, non-invasive monitoring of creatinine levels in interstitial fluid as an early indicator of AKI. The device integrates microneedle-based sampling with aptamer-functionalized electrodes and electrochemical sensing to achieve real-time measurements. Laboratory tests demonstrate the sensor's sensitivity and stability in detecting clinically relevant creatinine concentrations. The compact, portable design enables continuous monitoring, offering a pathway toward earlier intervention and improved patient outcomes in kidney care.

1 List of Abbreviations

- ABS – Acrylonitrile Butadiene Styrene
- AKI – Acute Kidney Injury
- BSA - Bovine Serum Albumin
- CE – Counter Electrode
- EDC – 1-ethyl-3-(-3-dimethylaminopropyl) carbodiimide hydrochloride
- EHR – Electronic Health Records
- FN – False Negative
- GDPR – General Data Protection Regulation
- GPIO - General Purpose Input/Output
- HDU – High Dependency Unit
- ICU – Intense Care Unit
- ISF – Interstitial fluid
- KDIGO – Kidney Disease: Improving Global Outcomes
- MCH – 6-mercaptohexan-1-ol
- MHA – 6-Mercaptohexanoic acid
- NaCl – Sodium Chloride
- NGAL – Neutrophil Gelatinase-Associated Lipocalin
- NHS – N-Hydroxysuccinimide
- PC – Personal Computer
- PCB – Printed Circuit Board
- PDMS – Polydimethylsiloxane
- PEG – Polyethylene Glycol
- PMCS – Post-Major Cardiac Surgery
- RE – Reference Electrode
- RRT – Renal Replacement Therapy
- SAM – Self-assembled monolayer
- SCR – Serum Creatinine
- SUS – System Usability Scale
- SWV – Square Wave Voltammetry
- TP – True Positive
- WE – Working Electrode
- UART – Universal Asynchronous Receiver/Transmitter
- ESP-IDF – Espressif IoT Development Framework

2 Analytical Performance award

The biosensor integrates an aptamer-based molecular recognition system with electrochemical transduction, implemented on a microfluidic chip and controlled via a compact PCB-powered reader device with a user-friendly web interface.

2.1 Molecular Recognition

The molecular recognition layer is designed to selectively detect creatinine, a key biomarker for monitoring kidney function. The recognition element of the biosensor is a 5'-amine, 3'-methylene blue aptamer (see Appendix 7.1), which was selected for its high specificity and high binding affinity to creatinine (Ganguly, Paul, & Prasad, 2023; Das, Raveendran, Bayry, & Rasheed, 2024). Aptamers offer a more robust alternative to antibodies due to their stability, modifiability and regeneration abilities (Idili, Gerson, Parolo, Kippin, & Plaxco, 2019), making them a good choice for continuous and wearable sensing. The functionalized gold surface (Figure 1) consists of a self-assembled monolayer (SAM) of 6-mercaptohexanoic acid (MHA) bound to a gold surface via S-Au bond formation, to which the aptamers and polyethylene glycol (48PEG or PEG) polymers are attached via amide bonds.

A MHA SAM was devised as an improvement on the thiolated aptamer with a 6-mercaptohexan-1-ol (MCH) backfilling system, which is typical for multiple aptamer-based biosensors (Lubin & Plaxco, 2010). This modification was inspired by reports that showed an increase in performance due to signal enhancement when carboxylate-terminal molecules were present on the surface (Bakestani et al., 2025). For this step, the packing density of the MHA on the surface was varied by adjusting the concentration (ionic strength) during the SAM formation.

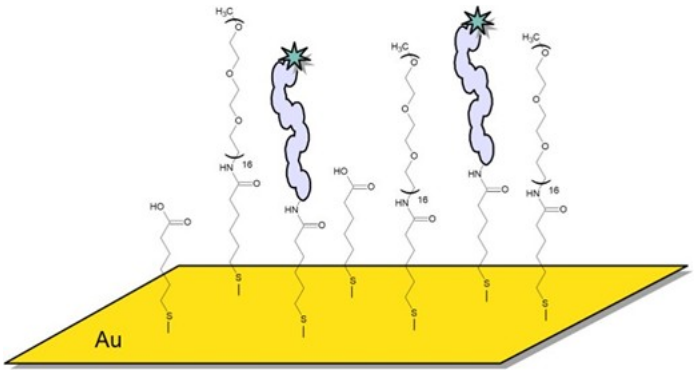

Figure 1: Functionalization of electrode surface

Then, and the aptamer were simultaneously attached to the carboxylic acid terminal groups of the MHA through their amine terminal groups. For this purpose, / was used as a binding agent (Fischer, 2010). The PEG on the surface is implemented as an antifouling layer to prevent non-specific adsorption of biomolecules that could be present in the interstitial fluid (ISF) complex media (Song, Han, Yu, Li, & Luo, 2024). ISF is formed through blood transcapillary filtration and shares 79% common components with blood and has similar concentration and dynamics (Zheng, Zhu, Xiao, Zheng, & Chen, 2023). This makes an attractive alternative source for biomarker detection.

2.2 Physical Transduction

The transduction relies on an electrochemical signal generated by the redox activity of the methylene blue tag covalently attached to the aptamer, typically measured using square wave voltammetry (SWV). The binding of creatinine to the aptamer induces a conformational change of the DNA strand that shifts the relative position of the methylene blue from the surface (Z. Hu et al., 2023; G. Wang et al., 2017; Wu et al., 2022). This affects the electron transfer between the electrode and the methylene blue, diminishing the current for the creatinine-bound state. The transduction method consists of the use of SWV (Z. Hu et al., 2023; Wu et al., 2022) and detection of the peak current at the methylene blue redox potential, which is correlated to a concentration with a calibration curve. To allow for the SWV measurements, a three-electrode set-up was implemented in the chip, with a functionalized gold WE, a gold CE, and a silver-silver chloride RE.

2.3 Cartridge Technology

To obtain the SWV signal, it is necessary to design a sensing chip with a microfluidic channel, for the sample to flow through the chip; the RE positioned at the inlet and the outlet of the chip; the WE located at the site where aptamers are functionalized for sensing; and CE. The design of the chip was done using Clewin Software, with the objective of minimizing the chip size while having the largest WE surface possible. To achieve this, a serpentine-shaped microfluidic channel was adopted, with a WE width of 400 μm, CE width of 100 μm, and a constant separation between both of 100 μm. This design ensures a reliable signal across the entire channel length. The final calculated areas for each electrode and the specific dimensions of each element of the chip are presented in Table 4 and Figure 8. Each chip was designed with final dimensions of 1.13 cm × 1.00 cm, allowing us to fit 116 chips per wafer as seen in Figure 9. The concept design of the chip is seen in Figure 2.

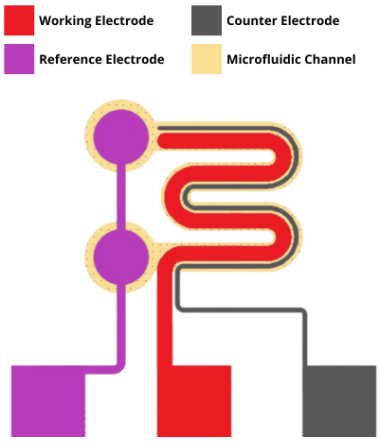

Figure 2: Design of the Chip with its the different components

2.4 Reader Instrument and User Interaction

This section describes the hardware, software, and user interactions of the reader instrument, with a focus on practical handling and ease of use.

The device's hardware is organized on a PCB we designed ourselves. The final goal is to make the sensor wearable; consequently, the design of the PCB should be small, power-efficient, easy to configure, and able to operate completely wirelessly. This PCB contains everything needed to interface with the electrochemical cell, set measurement modes (SWV), and transmit data wirelessly or through a cable to an external device which performs the necessary computations for diagnostics. The PCB potentiostat used is an EmStat Pico (PalmSens, n.d.-a), while the microcontroller is an ESP32 C3 Mini 1 (Systems, n.d.-a), equipped with an integrated wireless module. A key feature of the hardware is its ability to operate independently, powered by a LiPo battery. When

connected with a USB-C cable, it charges the battery and supplies power to the entire circuit simultaneously. The board measures 71 mm by 35.5 mm, with the antenna extending the length to 76 mm. The schematics of the PCB are provided in Section 7.4 and Figure 12, while the layout is shown in Figure 13. Note that in future developments, the dimensions could be significantly reduced, as further explained in Section 3.2.1.

The software is divided between the PC and the embedded system. The ESP32 acts as a UART bridge between the PC and the EmStat Pico, which performs measurements using PalmSens's MethodSCRIPT language (PalmSens, n.d.-b). The ESP32 is programmed in C using the ESP-IDF toolchain (Systems, n.d.-b) and only forwards data, keeping power consumption low. Python scripts on the PC handle sending commands, parsing responses, and displaying results. A web interface hosted on the ESP32 allows users to start SWV measurements, view live plots and monitor peak currents, thus monitoring creatinine levels in real-time (Figure 3). Once the measurement is stopped, the data can be downloaded in CSV format.

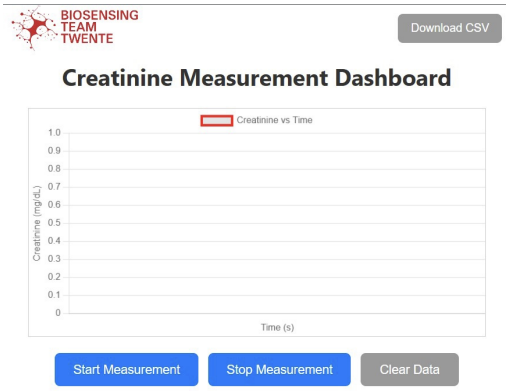

Figure 3: UI with Start/Stop for SWV measurement, Clear data, Download CSV; real-time creatinine vs. time plot.

The device is composed of two main parts: the measurement unit and the computer interface. To provide a clearer picture, Figure 11 in Section 7.4 shows an overall schematic of the working system. The measurement unit includes all the hardware components (pump, electronics, electrochemical sensor), while the computer interface provides real-time visualization and control via a web-based platform. From the user's perspective, the operation is minimal and straightforward, involving just two main steps. First, the sample must be deposited into a funnel-shaped inlet designed to minimize dead volume and ensure smooth fluid flow. This inlet connects directly to the input of the pump, which is powered via a standard power plug. Then, the user activates the Reglo-Z Digital pump (Ismatec) to drive the sample through the device. Once activated, the pump delivers the sample to the microfluidic chip, which has been functionalized with aptamers. This chip is connected to the PC, where all signal processing is performed. After analysis, the sample is directed into a waste reservoir. The user interface is minimal and designed for accessibility, requiring no installation. It can be accessed from any device on the same network, offering real-time visualization of the measurements and control over the device.

3 Innovation Award

3.1 Wearable Sensor

Our team has developed a wearable biosensor designed to continuously measure creatinine levels in ISF. This innovative device integrates modular hardware design, optimized surface chemistry, and custom low-power electronics, ensuring a compact, user-friendly, and reliable solution. The biosensor consists of two main modules: a disposable sensing patch which rests in the lower casing and a reusable electronics module which rests inside the upper casing as seen in the exploded view. The design emphasizes usability, robustness, and biomedical compatibility to deliver accurate, real-time data without compromising patient comfort or safety.

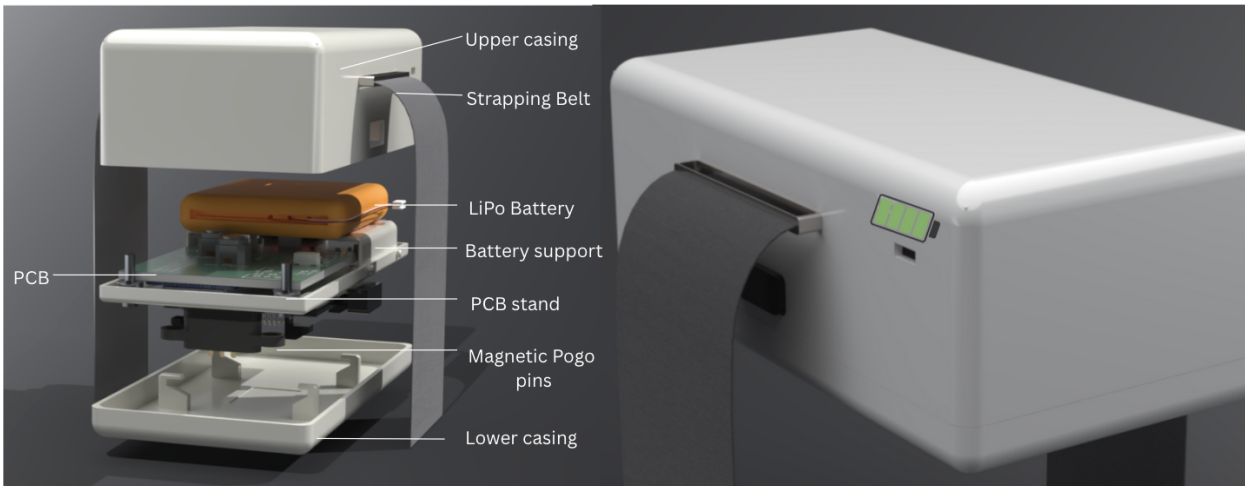

Figure 4: Exploded view of the wearable sensor and overall casing

3.1.1 Technological Novelty of Wearable Sensor

The wearable sensor introduces several novel technological aspects. The lower, disposable module features a microneedle-based sensor chip designed for stable electrochemical signal acquisition, as detailed in Section 2.3. It is designed with microneedle geometry (Figure 10), resting on a with a surface area of $6\,\mathrm{mm}^2$, to painlessly penetrate the stratum corneum and access ISF directly. Although this microneedle structure has not yet been fabricated, its design is supported by existing literature and will be pursued in future work (Zheng et al., 2023). A removable protective film maintains sterility before use, ensuring safety and aptamer longevity (Figure 5 (a)).

The reusable upper module integrates critical electronics, including a custom , LiPo battery, power management, and signal processing module (Figure 5 (b)). Connection to the sensor chip is achieved via four centrally positioned magnetic pogo pins, ensuring stable alignment and reducing signal loss due to mechanical stress or misalignment. This detachable interface (Figure 5 (c)) allows in reducing electronic waste and cost per cycle.

The device features an ergonomic, user-focused design with visual indicators that provide real-time feedback on attachment status and battery levels, making application straightforward. Its biosensor mechanism, inspired by a cantilever snap-fit, uses two L-shaped clamp arms that slide

along the X-axis and are pushed outward by compression springs. Pressing the arms inward compresses the springs, disengaging the snap-fit between the upper and lower casings so the bottom casing can be removed or replaced. For secure wear, a fabric belt straps the biosensor to the user's arm, while an adhesive layer on the bottom of the lower casing ensures stable positioning. Together, these elements enable continuous monitoring through consistent skin contact, reliable signal capture, and modular reusability. The novelty lies in integrating molecular recognition, physical transduction, and intuitive user interaction into a flexible, wearable platform.

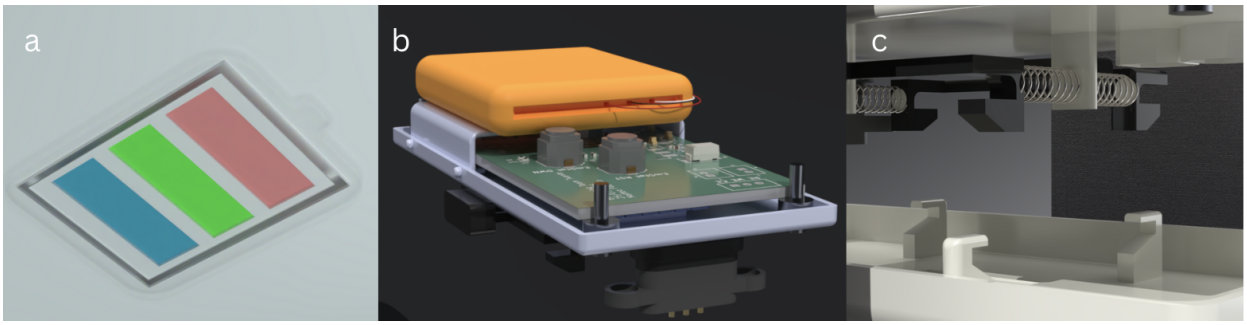

Figure 5: (a) Microneedle surface and film. (b) Reusable upper module. (c)Spring activated cantilever snap fit mechanism.

3.1.2 Technical Feasibility of Wearable Sensor

To ensure safety, reliability, and comfort in a hospital environment, the device must meet specific material requirements for use over 48 hours in settings like s, s, and recovery wards. The materials must offer high impact resistance, dimensional stability, and flexibility to endure bending without cracking. Thermal properties are critical, with low thermal conductivity to protect the skin from internal heating and stability under moderate temperature increases. The casing should be ergonomic, with smooth edges and a neutral medical colour palette. The skin-contacting area remains within $10 \times 10\cdot$ cm to preserve comfort. All contact materials are theoretically chosen to comply with ISO 10993 standards for biocompatibility and hypoallergenicity (*Biological evaluation of medical devices – Part 23: Tests for irritation*, 2021). According to MDR Annex VIII Rule 10, the device, an active instrument intended for continuous diagnosis and monitoring of creatinine levels, would be classified as a Class IIa medical device (Medical Device Coordination Group (MDCG), 2021).

For the microneedle patch, we propose 3M Medical Tape 4576 (Solventum / 3M Company, 2025) due to its extended-wear acrylate adhesive and soft spunlace polyester backing, providing strong skin adhesion with low moisture exchange. For the housing, Acrylonitrile Butadiene Styrene () was selected based on its impact resistance, light weight, and suitability for injection molding (SpecialChem, 2025). Although the microneedles have not been physically produced, the functionalization strategy was verified in vitro on gold wafers using the same chemistry. The assembly of a SAM via the Au-S bond formation has been reported in literature for mixed MCH (Lubin & Plaxco, 2010; Idili et al., 2019) and MCH/MHA (Bakestani et al., 2025) with thiolated aptamers. Furthermore, the formation of the amide bond between the carboxylic acid and amine functional groups using the / chemistry is a process commonly employed in biological applications

(Fischer, 2010). A functionalization of a gold surface described in the Section 2.1 was monitored using Quartz Crystal Microbalance (QCM) measurements (Figure 23 and 22), showing the successful attachment of each layer to the chip, with each reagent being continuously supplied via microfluidic channels.

A custom PCB has been developed for analog signal conditioning, digital processing, and real-time wireless communication. The compact design is energy-efficient and supports seamless integration with hospital systems and Electronic Health Records (EHRs), enabling timely clinical responses (Section 4.2).

3.2 Reliability of Sensor Output

3.2.1 Technological Novelty of Reliability Concept

The reliability of the sensor output is ensured through the integration of multiple design elements spanning molecular chemistry, hardware, and signal acquisition. The molecular recognition strategy follows the structure detailed in Section 2.1, but incorporates innovations to improve long-term stability and specificity. The use of a mixed PEG-aptamer layer covalently bonded via / chemistry enhances antifouling properties, limiting nonspecific adsorption from other molecules in (Song et al., 2024). The incorporation of MHA further improves electrochemical signal intensity due to its carboxylate terminations (Bakestani et al., 2025). Electrochemical sensing is performed using (SWV), which offers high sensitivity and is compatible with surface-confined redox reporters like methylene blue (PalmSens, 2022).

From a hardware perspective, the custom integrates analog front-end electronics, digital processing, and wireless transmission, ensuring low noise and fast signal acquisition. The system currently uses an ESP32 C3 Mini 1 microcontroller for its ease of integration and low-power capabilities. It is important to note that this board was developed as a prototype, so several extra features have been included for flexibility during testing. A GND pin and 3V3 pin, as well as many of the ESP32's general purpose input/output () pins, are accessible from outside the board, to power and control eventual additional external devices. Additionally, multiple switches are provided to isolate specific parts of the circuit to make debugging easier. These added features make the prototype larger than what a final, industry-ready product would require. With further optimization and by removing the extra debug and prototyping components, the size could be made smaller.

Although the ESP32 C3 Mini 1 is a solid choice, there are more advanced solutions available for industry applications. For example, microcontrollers from Nordic Semiconductor, such as the nRF52 or nRF53 series, are widely used for their ultra-low power consumption and highly efficient wireless modules. These alternatives can offer longer battery life, stronger wireless performance, and a smaller footprint, making them ideal for products intended for large-scale manufacturing and commercial deployment.

In terms of the software, the novelty lies in combining low-power hardware with PC-based data processing and a simple web interface. The ESP32 only forwards data, which ensures that the raw measurements from the potentiostat are transmitted without modification. This setup im-

proves reliability compared to fully embedded systems, while the web interface allows real-time monitoring and CSV export for further clinical analysis.

3.2.2 Technical Feasibility of Reliability Concept

Aptamers have been shown to generally bind reversibly to the target (Dief, Tang, Carroll, Breton, & Gooding, 2025), and the used sequence to bind specifically to creatinine(Ganguly et al., 2023; Das et al., 2024), and the methylene blue reporter is common for electrochemical aptasensing applications (Lubin & Plaxco, 2010). The verification of the presence of the methylene blue reporter was done via SWV after functionalization of gold wafers with dip coating procedures for different aptamer-PEG ratios (Figure 24).

Additionally, the signal appears to be sensitive to the creatinine concentration, as shown in Figure 6. The core sensing chemistry has been validated by research for biocompatibility (J. Wang et al., 2024; Ludovica Parisi, 2017), ensuring safe skin contact. Our chemical components are all individually stable under physiological conditions (Song et al., 2024) for our use case, and our chemistry is adaptable to microneedle-based contact (Wu et al., 2022; Zheng et al., 2023), ensuring continuous diffusion of ISF to the sensor. Preliminary lab results indicate sensitivity and selectivity for creatinine (Figure 6).

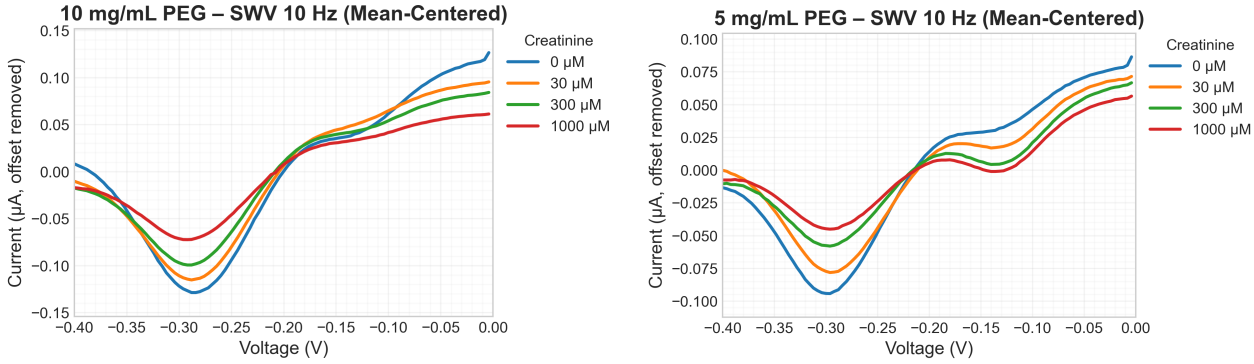

Figure 6: SWV results for the sensing signal at different creatinine concentrations for different wafers functionalized with different PEG concentrations. The SWV plots were measured at a frequency of 10 Hz.

The operation of the sensor is based on microneedle-enabled electrochemical detection using aptamers specific to creatinine. The critical elements of the system include: the stability and responsiveness of the aptamers, the reliability and quality of the materials used for better signal to noise ratio and signal quality, the geometry and layout of the microneedle electrodes for signal capture, the precision of the SWV readout method, and the mechanical-electrical interface that ensures signal fidelity between the detachable sensing patch and the reusable electronics.

A prototype chip was fabricated with a three-electrode configuration and tested in vitro using standard creatinine solutions. Preliminary results showed a correlation between peak current and creatinine concentration (Figure 25).

In summary, while some elements—such as long-term in vivo stability—require further testing, the combination of aptamer-based recognition, stable chip signal capture, and robust circuit integration presents a strong basis for a wearable sensor capable of delivering clinically reliable creatinine concentrations. Our simulation and early experimental data suggest that the proposed concept is technically feasible and scalable with further refinement.

3.3 Original Contributions

3.3.1 Team Piece

Our team began the biosensor development process with an in-depth literature review on microneedle-based sensing, antifouling chemistries, and electrochemical detection methods. Aptamer-based electrochemical sensing was identified as the most promising approach for reliable AKI monitoring, and optimized it with a novel PEG–aptamer mixed layer to enhance antifouling properties and signal stability, which was suggested by the supervisors and then tested and integrated by the team..

The concept of integrating this chemistry into a modular wearable device, with a disposable sensing patch and a reusable electronics module, was conceived, selected, and refined entirely by the team. We designed the chip layout, developed the custom , and determined material choices based on both biomedical compatibility and mechanical requirements. The electrochemical SWV method was selected for its compatibility with the antifouling layer and surface-based sensing, directly influencing chip design. The serpentine microfluidic layout was developed to support stable signal output, with technical input from Mohammad Saghafi.

All surface functionalization, QCM verification, and SWV sensing tests were planned and executed by the team, ensuring that the device design, molecular recognition strategy, and electronics integration were validated in-house. The wearable and modular design of the system, along with the integration of the chip, pump, and EmStat Pico, were completed independently, with supervisors providing targeted technical guidance rather than direct design control.

Queralt Piferrer & Timur Djalilov

3.3.2 Supervisor Piece

General information on type of coatings, and type of sensors/sensing techniques has been provided by the supervisors in the form of papers. The students have gathered additional information to assure a complete overview of the different options before making a decision. Practicalities with some sensing techniques and/or coating strategies have been provided if the supervisors were familiar (for example, pricing, easiness of handling, complexity). The students have decided independently on the best strategy for type of sensing technique and coating based on the provided information.

The starting point for protocols for surface functionalization were provided if available, but these were adjusted accordingly by the students. Protocols for the QCM-D were a combined effort of the supervisors (on speeds, volumes etc.) and the students (concentrations, specific chemicals,

order of steps). Regarding the Translation Potential section, the team was proactive in researching and selecting market segments in line with their envisioned competitive edge. The role of the supervisor was limited to help them to structure and communicate their thought and strategical choices.

4 Translation Potential Award

AKI is a sudden loss of kidney function that can progress rapidly to failure if not detected and treated early. Over 50% of ICU patients develop stage 1 , with fewer progressing to stages 2–3, and about 10% requiring (Hoste & Kellum, 2018). Detection is often delayed because , the standard biomarker, rises only 24–72 hours after injury, and current protocols rely on intermittent blood draws. Surgical patients undergo an average of 116 blood tests per stay (Society of Thoracic Surgeons, 2015), increasing discomfort, infection risk, and costs. Postoperative adds an average $15,800 per patient, with severe cases exceeding $40,000 (Hobson et al., 2015a; Silver, Long, Zheng, & Chertow, 2017). Late detection is associated with in-hospital mortality of 10.7%, long-term mortality up to 30% (Corredor, Thomson, & Al-Subaie, 2016; Chen, Wang, Liu, et al., 2018), and prolonged ICU/hospital stays that further strain resources.

4.1 Customer Interviews

In order to gather design requirements for the device, we conducted interviews with stakeholders such as nephrologists, nurses, and experts who are involved with , cardiac surgery, or kidney specialists. Messages were sent to these stakeholders found through LinkedIn, the University connections, etc. An interview was set, and questions that were deemed relevant to their expertise were asked during the interview. A full list of the professionals interviewed can be found in Appendix 4.1.

4.1.1 Summary of Insights

Expert consultations and literature review identified patients as the optimal group for device testing. While is common in sepsis, pre-existing kidney impairment often limits early detection benefits. In contrast, patients typically develop postoperatively, providing a clearer intervention window. Cardiac surgery compromises renal perfusion via artery clamping or cardiopulmonary bypass, raising risk, with incidence ranging from 19% in coronary bypass to 29% in aortic surgeries (Vandenberghe, Gevaert, Kellum, et al., 2016; J. Hu, Chen, Liu, et al., 2016), and overall rates up to 30% (Vives et al., 2019). This high postoperative incidence and defined onset make patients ideal for early detection.

Stakeholders	Needs	Concerns
Patients	Continuous, non-invasive kidney monitoring to reduce blood draws, especially for chronic or post-transplant patients. Early detection can improve quality of life and prevent complications.	Reliability and comfort of wearables, psychological impact of continuous monitoring, and risk of false alarms.
Nephrologists	Target groups include post-cardiac surgery and sepsis patients, with many septic cases presenting in emergency or ward settings.	All three groups note that serum creatinine is a late, unreliable biomarker—levels often rise only after significant kidney damage has occurred.
Nurses	Minimize or eliminate blood draws to reduce clot risk and enable use in dialysis patients. Device should be easy to change and not interfere with other treatments.	
Experts (AKI specialists, endocrinologists, cardiac surgeons, etc.)	Best suited for patients at high AKI risk: post-cardiac surgery, kidney transplant recipients, those on nephrotoxic drugs, or recovering from infection. Placement should avoid joints (e.g., arm, thigh, abdomen).	

Table 1: Insights from stakeholder interviews.

Moreover, it became clear that relying solely on creatinine is a limitation because it is a delayed biomarker of kidney injury. To address this, we explored the inclusion of neutrophil gelatinase-associated lipocalin (NGAL), which rises within hours after renal tubular injury and allows earlier AKI detection compared to creatinine (Hoste & Kellum, 2018). (Yang, Gan, Song, Yuan, & Xiang, 2022) have demonstrated sensitive aptamer-based electrochemical biosensors for NGAL detection. Since our device already employs aptamer chemistry, NGAL detection could be integrated by modifying the chip surface, allowing multiplexed detection without altering the overall sensing platform design.

In addition to clinical needs, stakeholders highlighted potential risks and usability concerns related to the device. Table 2 below summarizes the most critical hazards mentioned by stakeholders, while the full hazard matrix is presented in Appendix 7.8.

Hazard	Description	O	S	D	RPN
Detachability	Patch may detach from skin due to sweating or movement.	4	6	8	192
Alarm missed	Nurse fails to hear the alarm after creatinine rise, delaying intervention, hence the device is useless.	6	10	9	540
Data Transfer	Wireless transmission to EHR may fail or be delayed.	5	7	5	175
Device Malfunction	Internal component failure (e.g., sensor, battery) halts operation.	4	9	8	288
Sensitivity (False Negatives)	Alarm is not triggered even though the patient is in danger.	6	9	8	432

Table 2: Hazard traceability matrix with color-coded (values form 1-10) Occurrence (O), Severity (S), and Detection (D) levels, based on defined risk ranges.

Moreover, a critical point which was gathered for introducing a new device to a hospital is to keep the adaptation cost minimal, and the device must not disrupt the current workflow of the hospital, shortly found in the Patient Journey of Figure 21 in the Appendix. As a result, the data will be sent wirelessly directly to the Electronic Hospital Record immediately.

4.2 Design of Validation Study

A mock-up simulating key device functions will be used to test integration and usability in a clinical setting without requiring a fully developed prototype. We hypothesize that continuous real-time sCr monitoring with a minimally invasive biosensor will enable earlier AKI detection than intermittent lab testing, leading to faster intervention, fewer undiagnosed cases, and improved outcomes. PMCS patients, who have high AKI incidence and unmet need for early detection as explained in 4.1, are selected as the primary validation group.

The validation study will assess both the clinical benefit of earlier AKI detection and the usability of the device in real workflows, focusing on workflow compatibility, ease of use for healthcare providers, and patient comfort. The key questions are:

1. Does real-time sCr monitoring allow for earlier detection of AKI compared to standard intermittent blood testing?
2. Is the device comfortable for patients, easy for healthcare providers to use, and compatible with current clinical workflows?

This pilot multi-center observational study will be conducted at UMC Utrecht, Erasmus MC Rotterdam, and Amsterdam UMC, selected for their high cardiac surgery volume and expertise in research and device innovation. The study will adhere to Good Clinical Practice (), the General Data Protection Regulation (), and the Declaration of Helsinki (European Medicines Agency, 2023; World Medical Association, n.d.; *General Data Protection Regulation*, 2016).

Participants

Patients over 18 years admitted for cardiac surgery between September 2025 and February 2026, with an expected hospital stay of at least one week, are invited to participate. Approximately **94 patients** will be recruited across three hospitals, based on the sample size calculation in Appendix 7.10.

ICU nurses, nephrologists, and cardiothoracic surgeons with at least 2 years of experience and currently employed at participating hospitals will also be included for usability and workflow testing. A minimum of **30 practitioners** (10 per hospital) will ensure diverse clinical perspectives. Detailed inclusion and exclusion criteria for patients and practitioners are provided in Appendix 7.11.

Protocol

The biosensor will be applied preoperatively to establish a baseline value and will remain in place throughout surgery and the postoperative period, as illustrated in Figure (*to be designed*). The device is not expected to interfere with surgical or postoperative care. Suspected events, identified using KDIGO-aligned thresholds (Kidney Disease: Improving Global Outcomes (KDIGO), n.d.), will trigger confirmatory blood tests via the hospital's standard lab method, harmonized across all study sites. Detailed protocols for data processing and storage are outlined in Appendix 7.12.

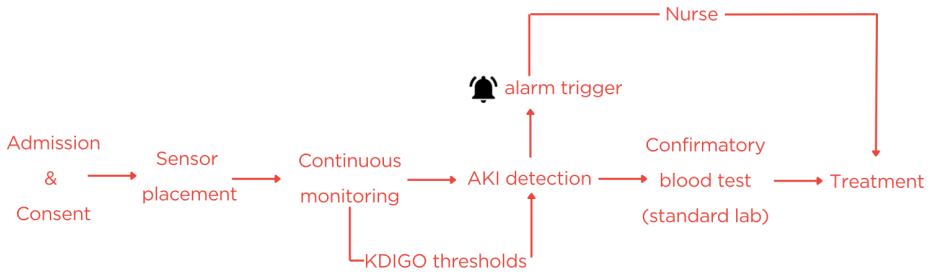

Figure 7: Flowchart of the study protocol and monitoring process

Data Collection and Event Classification

Upon a biosensor alarm, a nurse will draw blood within 30 minutes to measure serum creatinine (reference method). Sensor and lab results, along with timestamps and alarm metadata, will be

logged in the EHR. A nephrologist will then review the paired data to confirm or rule out . If confirmed, treatment follows the Dutch hospital protocol. Independent of alarms, routine morning lab draws are performed to capture any missed events. This workflow enables classification of events as true positives (), false positives (FP), false negatives (FN), or true negatives (TN), allowing calculation of sensitivity, specificity, PPV, and NPV. The goals for these performance metrics are discussed in the Appendix 7.15.

The device will record creatinine every 30 minutes, with all data stored in the EHR and later exported to a secure research database in accordance with institutional policy. Collected variables include:

- **Biosensor:** hourly sCr readings, alarm status, timestamps, error logs.
- **Lab reference:** sCr from EHR (routine standard draw for lab diagnosis and triggered draws).
- **Clinical outcomes:** AKI stage, ICU/hospital LOS, requirement, and mortality.
- **Operational and Usability:** response time, missed alarms, protocol adherence, nurse and patient System Usability Scale (SUS) scores through surveys.

For each event, the detection time advantage is calculated as:

$$\Delta T = T_{\text{lab diagnosis}} - T_{\text{biosensor alarm}}$$

where $T_{\text{lab diagnosis}}$ is the time of blood draw or EHR entry, depending on institutional standards. The mean ΔT represents the average time gained in AKI detection, a key metric for quantifying the device's clinical and economic value.

Usability evaluation via standardized questionnaires (System Usability Scale - SUS) completed by nurses and patients.

4.3 Expected outcomes

If successful, the continuous creatinine-based biosensor will enable earlier detection of AKI in cardiac patients, preventing progression to severe stages in an estimated 20–30% of high-risk cases (Hoste & Kellum, 2018). In the Netherlands, with approximately 15,000 adult patients undergoing CABG or valve surgeries annually (van Straten et al., 2014), this could prevent severe AKI in around 3,000–4,500 patients each year. Given that each prevented case can save €1,500–2,000 per ICU day (Alshaikh et al., 2018) and avoid 3–7 extra days in critical care (Hobson et al., 2015b), the potential healthcare savings range from €13.5 million to €63 million annually. Clinically, early detection could reduce in-hospital mortality by 3–5 percentage points (Corredor et al., 2016) and long-term mortality by up to 10 percent (Chen et al., 2018), while also decreasing the incidence of chronic kidney disease and the need for dialysis. The device adds further value by reducing reliance on frequent blood draws, minimizing infection risk, and improving ICU workflow efficiency. Expected performance metrics from the validation study are discussed in the Appendix 7.14.

5 Team and support

5.1 Team Contributions

Name	Contributions
Andrea	Molecular recognition and transduction design; QCM, electrochemistry, and chip functionalization and cleaning; created related protocols; social media and merchandising.
Fernando	Molecular recognition and transduction design; QCM, electrochemistry, and chip functionalization and cleaning; helped standardize protocols.
Vicent	Molecular recognition and transduction design; QCM, electrochemistry, and chip functionalization and cleaning; data processing and analysis.
Jan	Device design; pump selection and tuning; team website.
Marc	Microfluidic chip design; CleWin layout; team website.
Timur	Chip design and experiments; data analysis; team captain setting weekly team meetings, and overseeing various subteams.
Matteo	Designed custom PCB; integrated electronic components.
Aakriti	EmStat Pico-chip connection to the chip; user-facing website development.
Sarah	Customer interviews; stakeholder contact; device design.
Paulo	Customer interviews; device design concepts and implementation; clinical validation study
Deikshi	Customer interviews; wearable design concepts and 3D model; social media and merchandising.
Sreya	Social media and merchandising.
Queralt	Customer interviews; clinical validation study; wearable design; team captain liaising with board members and supervisors, setting weekly team meetings, and overseeing various subteams.

Table 3: Overview of individual team member contributions.

5.2 Supporters

Board Members

- Diana – External communication, lab access.
- Jan Pieter – EmStat Pico intro, chip manufacturing support.
- Danail – Sponsor outreach, business case support.
- Caterina – Social media and events.
- Vinaya – Event planning, budget management.

Supervisors

- Mohammad – Chip design, process flow.
- Jannis, Amarna, Hanna – Chemistry lab guidance.
- Pep – Business case and coordination support.

External Contributors

- Daniel Wijnperle – Chip manufacturing support at MESA+.
- Prof. Huskens from the MNF lab, and BIOS Prof. Segerink- Chemistry lab support and guidance.

5.3 Sponsors and Partners

- **Benchmark** – Workshops on PCB design, EMI/EMC; project support.

- **PalmSens** – Guidance on potentiostat design, MethodSCRIPT, PCB feedback.
- **MESA+ Institute** – Fabrication of the final chip design.
- **NovelT** – Legal, financial, and startup support; networking.
- **DeDesign** – Stakeholder brainstorming and device design support.
- **TechMed** – Problem refinement and exposure at university events.

6 Final remarks

We would like to thank everyone who has contributed to the development of our wearable biosensor over the past months for their valuable insights, time, and encouragement. This includes the SensUs organization and Jury, whose feedback sessions have been an essential support framework for our progress, as well as all the healthcare professionals who participated in our interviews and shared their expertise.

This journey has been both technically and personally transformative. As a team, we have navigated challenges ranging from design considerations to the optimization of our antifouling chemistry, and in doing so, we have grown in teamwork, problem-solving, and resilience. Our diverse academic and cultural backgrounds not only helped us tackle the multidisciplinary aspects of the project, but also made the process rewarding and enjoyable.

We are proud to present a concept that addresses the unmet need for continuous and reliable monitoring of AKI in high-risk patients. While further refinement will be required before clinical implementation, the device we have developed represents a strong foundation for future work, with promising extensions such as multi-biomarker detection.

Finally, we are deeply grateful for the opportunity to take part in the SensUs competition and for the unwavering support of our supervisors, as well as the board members, who have guided us with expertise, encouragement, and trust in our independence from the very start.

References

Abbott Point of Care. (n.d.). *i-stat creatinine test.* Retrieved from https://www.globalpointofcare.abbott/us/en/product-details/apoc/istat-crea-us.html (Accessed on 2023-10-13)

Alshaikh, H. N., Katz, N. M., Gani, F., Nagarajan, N., Canner, J. K., Kacker, S., … Schneider, E. B. (2018). Financial impact of acute kidney injury after cardiac operations in the united states. *The Annals of Thoracic Surgery*, *105*(2), 469–475. doi: 10.1016/j.athoracsur.2017.10.053

Bakestani, R. M., Wu, Y., Glahn-Martínez, B., Kippin, T. E., Plaxco, K. W., & Kolkman, R. W. (2025). Carboxylate-terminated electrode surfaces improve the performance of electrochemical aptamer-based sensors. *ACS Appl. Mater. Interfaces*, *17*. doi: 10.1021/acsami.4c21790

Beaubien-Souligny, W., Benkreira, A., Robillard, P., Bouabdallaoui, N., Chassé, M., Desjardins, G., … Denault, A. (2018). Alterations in portal vein flow and intrarenal venous flow are associated with acute kidney injury after cardiac surgery: A prospective observational cohort study. *Journal of the American Heart Association*, *7*(19). doi: 10.1161/jaha.118.009961

Biological evaluation of medical devices – part 23: Tests for irritation. (2021). Retrieved 2023-10-13, from https://connect.nen.nl/Standard/Detail/3641628?compId=0&collectionId=0 (ISO 10993-23:2021)

Chalice Medical. (2023). *Brochure: Product details.* Retrieved from https://www.chalicemedical.com/wp-content/uploads/2023/04/MRK00006_A00_RS_brochure_DIGITAL.pdf (Accessed on 2023-10-13)

Chawla, L. S., Eggers, P. W., Star, R. A., & Kimmel, P. L. (2014). Development and standardization of a novel biomarker of acute kidney injury. *Clinical Journal of the American Society of Nephrology*, *9*(9), 1433–1442.

Chen, Q.-H., Wang, H.-L., Liu, L., et al. (2018). Effects of restrictive red blood cell transfusion on the prognoses of adult patients undergoing cardiac surgery: a meta-analysis of randomized controlled trials. *Critical Care*, *22*(1), 142. doi: 10.1186/s13054-018-2062-5

Corredor, C., Thomson, R., & Al-Subaie, N. (2016). Long-term consequences of acute kidney injury after cardiac surgery: a systematic review and meta-analysis. *Journal of Cardiothoracic and Vascular Anesthesia*, *30*(1), 69–75. doi: 10.1053/j.jvca.2015.07.013

Das, C., Raveendran, J., Bayry, J., & Rasheed, P. A. (2024). Selective and naked eye colorimetric detection of creatinine through aptamer-based target-induced passivation of gold nanoparticles. , *14*(46), 33784–33793. Retrieved 2025-08-08, from https://xlink.rsc.org/?DOI=D4RA06191H doi: 10.1039/D4RA06191H

Dief, E. M., Tang, W., Carroll, L. R., Breton, T., & Gooding, J. J. (2025). Preparation of electrochemical aptamer-based sensors: a direct aryl diazonium grafting approach. *Chemical Communications*, *61*. doi: https://doi.org/10.1039/d5cc00857c

European Medicines Agency. (2023). *Good clinical practice.* https://www.ema.europa.eu/en/human-regulatory-overview/research-development/compliance-research-development/good-clinical-practice. (Accessed: 2025-05-21)

Fischer, M. J. E. (2010). Amine coupling through EDC/NHS: A practical approach. In N. J. Mol & M. J. E. Fischer (Eds.), *Surface plasmon resonance* (Vol. 627, pp. 55–73). Humana Press. Retrieved 2025-08-08, from http://link.springer.com/10.1007/978-1-60761-670-2_3 (Series Title: Methods in Molecular Biology) doi: 10.1007/978-1-60761-670-2_3

Ganguly, A., Paul, A., & Prasad, S. (2023). Pysanka-inspired electrode modification with aptamer encapsulation in ZIF-8 for urine creatinine electrochemical biosensing. , *11*(11), 557. Retrieved 2025-08-08, from https://www.mdpi.com/2227-9040/11/11/557 doi: 10.3390/chemosensors11110557

General Data Protection Regulation. (2016, April). https://eur-lex.europa.eu/legal-content/ES/TXT/?uri=CELEX:32016R0679. (Accessed: 2025-08-07)

Hobson, C., Ozrazgat-Baslanti, T., Kuxhausen, A., Thottakkara, P., Efron, P., Moore, F., & Bihorac, A. (2015b). Cost and mortality associated with postoperative acute kidney injury. *Annals of Surgery*, *261*(6), 1207–1214. Retrieved from https://doi.org/10.1097/SLA.0000000000000830 doi: 10.1097/SLA.0000000000000830

Hobson, C., Ozrazgat-Baslanti, T., Kuxhausen, A., Thottakkara, P., Efron, P. A., Moore, F. A., ... Bihorac, A. (2015a). Cost and mortality associated with postoperative acute kidney injury. *Annals of Surgery*, *261*(6), 1207–1214. doi: 10.1097/sla.0000000000000732

Hoste, E. A. J., & Kellum, J. A. (2018). Acute kidney injury in the icu: From injury to recovery. *Critical Care Medicine*, *46*(6), e537-e542. Retrieved from https://doi.org/10.1097/CCM.0000000000003119 doi: 10.1097/CCM.0000000000003119

Hu, J., Chen, R., Liu, S., et al. (2016). Global incidence and outcomes of adult patients with acute kidney injury after cardiac surgery: a systematic review and meta-analysis. *Journal of Cardiothoracic and Vascular Anesthesia*, *30*(1), 82–89. doi: 10.1053/j.jvca.2015.06.017

Hu, Z., Zhu, R., Figueroa-Miranda, G., Zhou, L., Feng, L., Offenhäusser, A., & Mayer, D. (2023). Truncated electrochemical aptasensor with enhanced antifouling capability for highly sensitive serotonin detection. *Biosensors*, *13*. doi: 10.3390/bios13090881

Idili, A., Gerson, J., Parolo, C., Kippin, T., & Plaxco, K. W. (2019). An electrochemical aptamer-based sensor for the rapid and convenient measurement of l-tryptophan. , *411*(19), 4629–4635. Retrieved 2025-08-08, from http://link.springer.com/10.1007/s00216-019-01645-0 doi: 10.1007/s00216-019-01645-0

Kashani, K., Al-Khafaji, A., Ardiles, T., Artigas, A., Bagshaw, S. M., Bell, M., et al. (2013). Discovery and validation of cell cycle arrest biomarkers in human acute kidney injury. *Critical Care*, *17*(1), R25.

Kellum, J. A., Lameire, N., Aspelin, P., Barsoum, R. S., Burdmann, E. A., Goldstein, S. L., et al. (2015). Diagnosis, evaluation, and management of acute kidney injury: a kdigo summary. *Critical Care*, *19*, 349.

Kidney Disease: Improving Global Outcomes (KDIGO). (n.d.). *Global science. local change.* https://kdigo.org/. (Accessed: 2025-05-21)

Koyner, J. L., Carey, K. A., Edelson, D. P., & Churpek, M. M. (2018). Performance of a machine learning model of acute kidney injury prediction. *NPJ Digital Medicine*, *1*(1), 24.

Lubin, A. A., & Plaxco, K. W. (2010). Folding-based electrochemical biosensors: The case for responsive nucleic acid architectures. , *43*(4), 496–505. Retrieved 2025-08-08, from https://pubs.acs.org/doi/10.1021/ar900165x doi: 10.1021/ar900165x

Ludovica Parisi, A. N. A. T. E. C. E. M. S. L. G. M. M. F. R. C. M., Carlo Galli. (2017). Aptamers improve the bioactivity of biomaterials. *Aptamers*, *1*. Retrieved from http://japtamers.co.uk/wp-content/uploads/2017/12/APT-01-03-Parisi.pdf

Mahlum, J. D., Pellitero, M. A., & Arroyo-Currás, N. (2021). Chemical equilibrium-based mech-

anism for the electrochemical reduction of DNA-bound methylene blue explains double redox waves in voltammetry. , *125*(17), 9038–9049. Retrieved 2025-08-08, from https://pubs.acs.org/doi/10.1021/acs.jpcc.1c00336 doi: 10.1021/acs.jpcc.1c00336

Medibeacon. (n.d.). *Medibeacon transdermal gfr system receives fda approval to assess kidney function.* Retrieved from https://www.medibeacon.com/medibeacon-transdermal-gfr-system-receives-fda-approval-to-assess-kidney-function/ (Accessed on 2023-10-13)

Medical Device Coordination Group (MDCG). (2021, October). *Guidance on classification of medical devices – MDCG 2021-24.* pdf document, European Commission. Retrieved from https://health.ec.europa.eu/system/files/2021-10/mdcg_2021-24_en_0.pdf (Accessed: 2025-08-08)

Nova Biomedical. (n.d.). *Statstrip creatinine.* Retrieved from https://www.novabiomedical.com/statstrip-creatinine/ (Accessed on 2023-10-13)

PalmSens. (n.d.-a). *Emstat pico module.* https://www.palmsens.com/product/oem-emstat-pico-module/. (Accessed July 26, 2025)

PalmSens. (n.d.-b). *Methodscript v1.5.* https://www.palmsens.com/knowledgebase-article/methodscript-v1-5/. (Accessed July 26, 2025)

PalmSens. (2022). *Square wave voltammetry (swv).* PalmSens Knowledge Base. Retrieved from https://www.palmsens.com/knowledgebase-article/square-wave-voltammetry-swv/ (Accessed August 6, 2025)

Silver, S. A., Long, J., Zheng, Y., & Chertow, G. M. (2017). Cost of acute kidney injury in hospitalized patients. *Journal of Hospital Medicine*, *12*(2), 70–76. doi: 10.12788/jhm.2683

Society of Thoracic Surgeons. (2015, March 2). *Frequency of blood tests in heart surgery patients may lead to anemia, transfusions.* https://www.sciencedaily.com/releases/2015/03/150302070759.htm. ScienceDaily. (Retrieved June 2, 2025)

Solventum / 3M Company. (2025). *3M™ Medical Tape 4576 – Technical Product Overview.* Web page, Solventum product listing. Retrieved from https://www.solventum.com/en-us/home/f/b5005369004/ (Accessed: 2025-08-08)

Song, Z., Han, R., Yu, K., Li, R., & Luo, X. (2024). Antifouling strategies for electrochemical sensing in complex biological media. , *191*(3), 138. Retrieved 2025-08-08, from https://link.springer.com/10.1007/s00604-024-06218-2 doi: 10.1007/s00604-024-06218-2

SpecialChem. (2025). *Acrylonitrile butadiene styrene (abs): Properties applications.* Retrieved from https://www.specialchem.com/plastics/guide/acrylonitrile-butadiene-styrene-abs-plastic (Accessed: 2025-08-08)

Systems, E. (n.d.-a). *Esp32-c3-mini-1 & mini-1u datasheet.* https://www.espressif.com/sites/default/files/documentation/esp32-c3-mini-1_datasheet_en.pdf. (Accessed July 26, 2025)

Systems, E. (n.d.-b). *Espressif-ide documentation.* https://docs.espressif.com/projects/espressif-ide/en/latest/index.html. (Accessed July 26, 2025)

Vandenberghe, W., Gevaert, S., Kellum, J. A., et al. (2016). Acute kidney injury in cardiorenal syndrome type 1 patients: a systematic review and meta-analysis. *Cardiorenal Medicine*, *6*(2), 116–128. doi: 10.1159/000442300

van Straten, A. H. M., Bekkers, J. A., Soliman Hamad, M. A., van Zundert, A. A. J., Martens, E. J., de Wolf, A. M., & ter Woorst, J. F. (2014). The netherlands association for cardio-thoracic surgery adult cardiac surgery database report 2010–2012. *Interactive CardioVascular and Thoracic Surgery*, *18*(5), 655–659. doi: 10.1093/icvts/ivt556

Vives, M., Hernandez, A., Parramon, F., Estanyol, N., Pardina, B., Muñoz, A., … Hernandez, C. (2019). lt;pgt;acute kidney injury after cardiac surgery: prevalence, impact and management challengeslt;/pgt;. *International Journal of Nephrology and Renovascular Disease*, 153–166. doi: 10.2147/ijnrd.s167477

Wang, G., Xu, Q., Liu, L., Su, X., Lin, J., Xu, G., & Luo, X. (2017). Mixed self-assembly of polyethylene glycol and aptamer on polydopamine surface for highly sensitive and low-fouling detection of adenosine triphosphate in complex media. *ACS Appl. Mater. Interfaces*, *9*. doi: 10.1021/acsami.7b09529

Wang, J., Shi, Y., Mao, B., Zhang, B., Yang, J., Hu, Z., & Liao, W. (2024). Biomaterials for inflammatory bowel disease: treatment, diagnosis and organoids. *Applied Materials Today*, *36*. doi: https://doi.org/10.1016/j.apmt.2024.102078

World Medical Association. (n.d.). *WMA Declaration of Helsinki – Ethical Principles for Medical Research Involving Human Participants.* `https://www.wma.net/policies-post/wma-declaration-of-helsinki/`. (Accessed: 2025-05-21)

Wu, Y., Tehrani, F., Teymourian, H., Mack, J., Shaver, A., Reynoso, M., … Arroyo-Currás, N. (2022). Microneedle aptamer-based sensors for continuous, real-time therapeutic drug monitoring. *Anal. Chem.*, *94*. doi: 10.1021/acs.analchem.2c00829

Yang, J., Gan, X., Song, X., Yuan, R., & Xiang, Y. (2022). Apamer-based sensitive and label-free electrochemical detection of neutrophil gelatinase-associated lipocalin via recycling amplification cascades. *Analytica Chimica Acta*, *1233*, 340515. doi: 10.1016/j.aca.2022.340515

Zheng, L., Zhu, D., Xiao, Y., Zheng, X., & Chen, P. (2023). Microneedle coupled epidermal sensor for multiplexed electrochemical detection of kidney disease biomarkers. *Biosensors and Bioelectronics*, *237*, 115506. doi: 10.1016/j.bios.2023.115506

7 Appendix

7.1 Aptamer Sequence

5’ Amino Modifier C6 - CGA-CGG-TGG-CCT-ATT-AAA-TAG-CTT-TAG-TTT-AAG-AAA-AGT-AAT-AGG-GGGTGT-CG - ATTO MB2 3’

7.2 Cartidage Technology Appendix

Table 4: Surface Areas of the Electrodes and Microfluidic Channel

Area (mm^2)	Working Electrode	Counter Electrode	Reference Electrode	Microfluidic Channel
Small Circle / Inlet	0.06	0.00	1.77	3.14
First Straight Line	1.13	0.28	0.00	2.25
First Small Arc	0.57	0.27	0.00	1.38
Second Straight Line	0.79	0.20	0.00	1.57
Second Big Arc	0.82	0.16	0.00	1.38
Third Straight Line	0.79	0.20	0.00	1.57
Third Small Arc	0.57	0.27	0.00	1.38
Fourth Straight Line	0.93	0.23	0.00	1.85
Fourth Arc / Outlet	0.31	0.02	1.77	3.14
Total Area	**5.95**	**1.62**	**3.53**	**17.68**

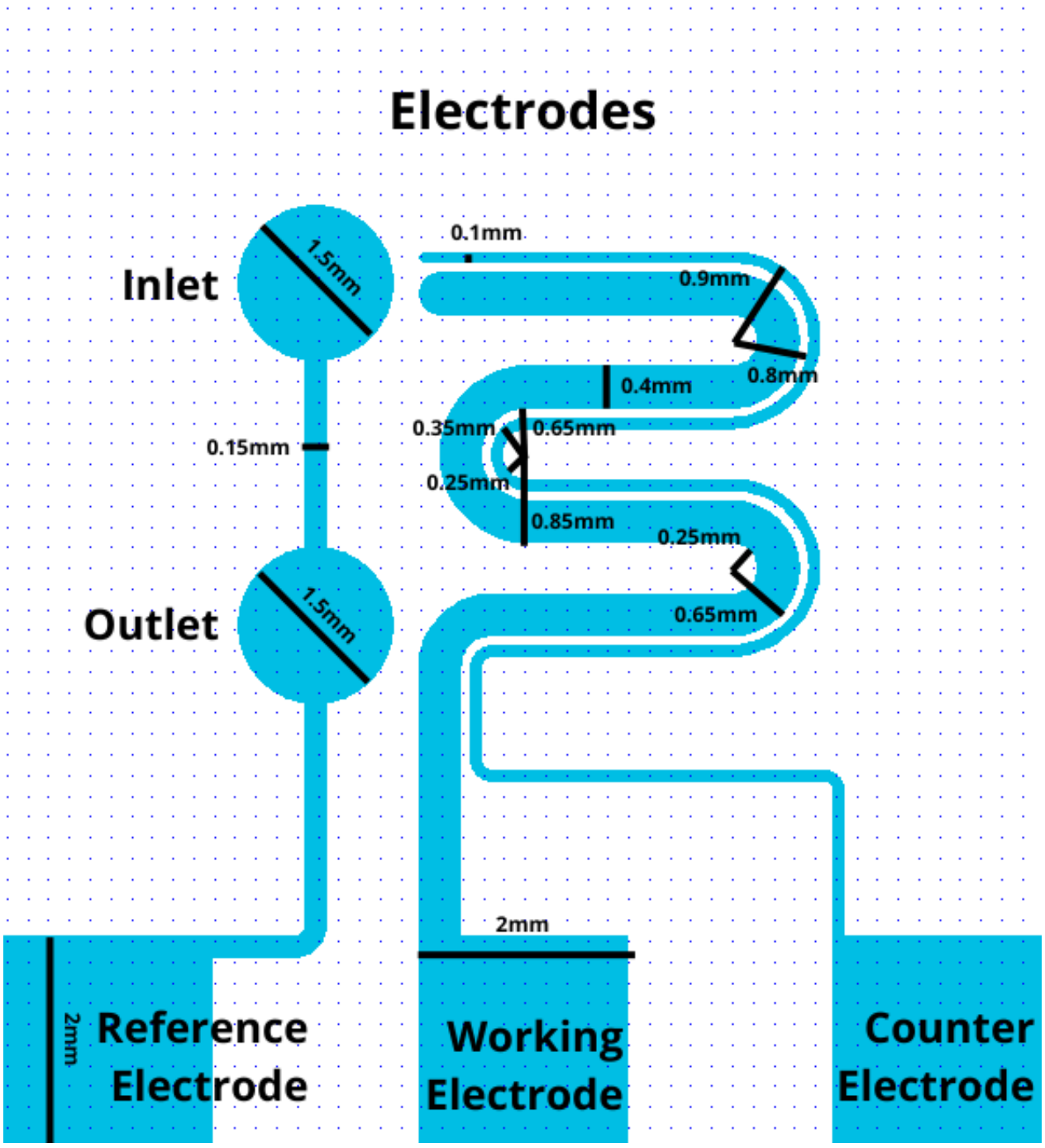
Electrodes
Inlet
1.5mm
0.1mm
0.9mm
0.8mm
0.4mm
0.35mm
0.65mm
0.25mm
0.85mm
0.25mm
0.65mm
0.15mm
Outlet
1.5mm
2mm
2mm
Reference Electrode
Working Electrode
Counter Electrode

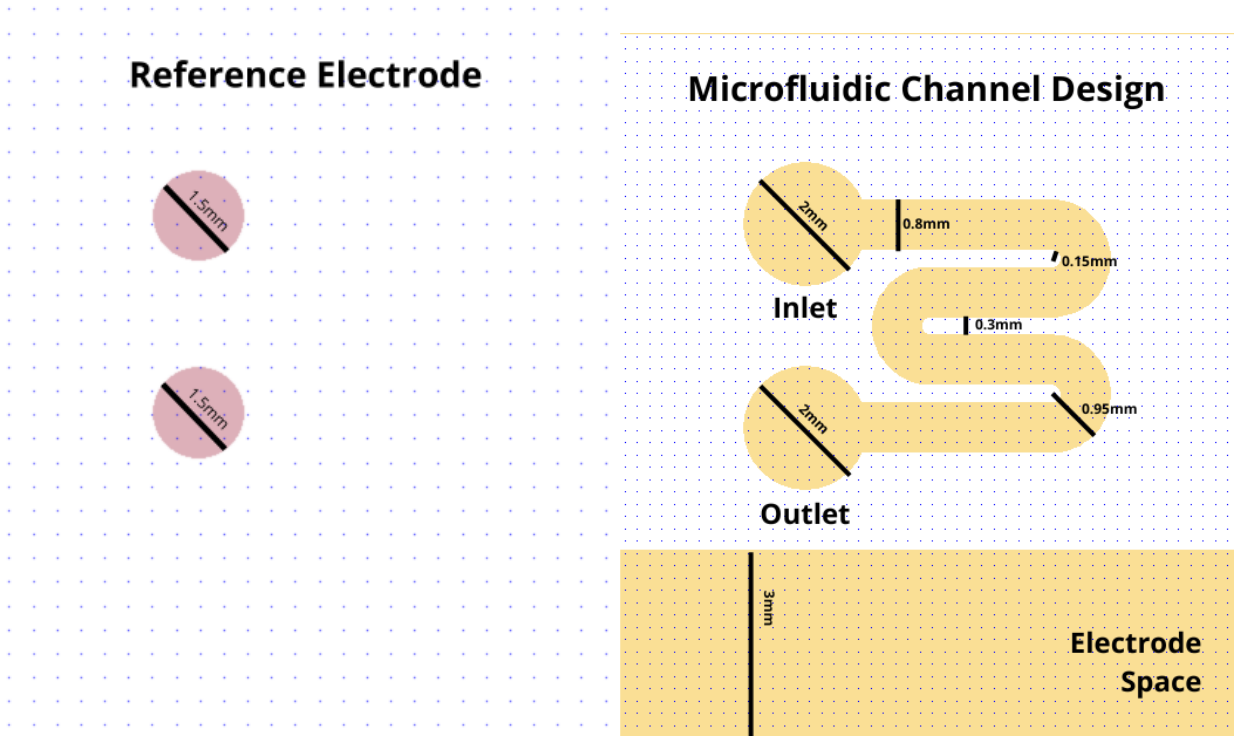

Figure 8: Figures of the three different layers of the Chip with its dimensions annotated

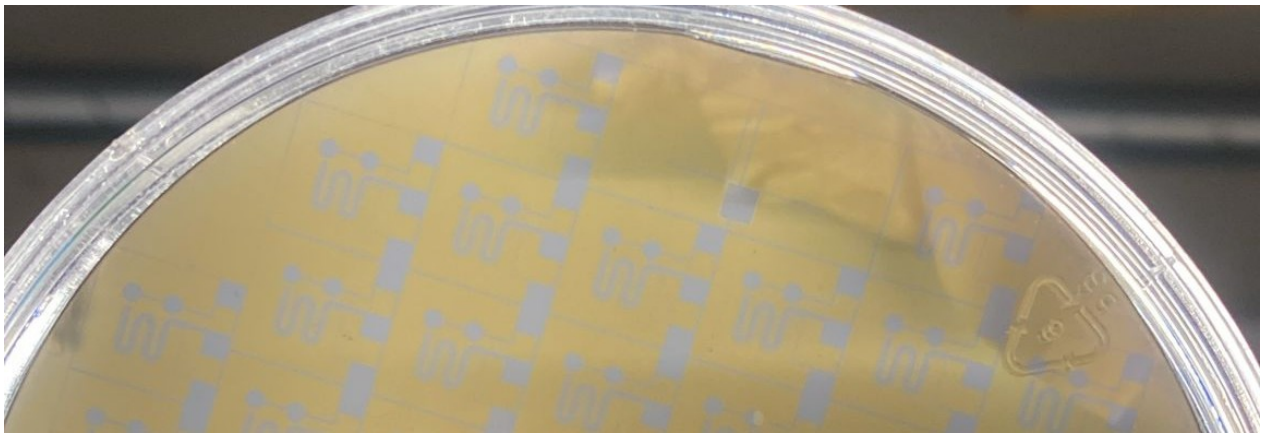

Figure 9: Picture of the Printed Chips that will be used during the Testing Event

7.3 Microneedle Chip Concept

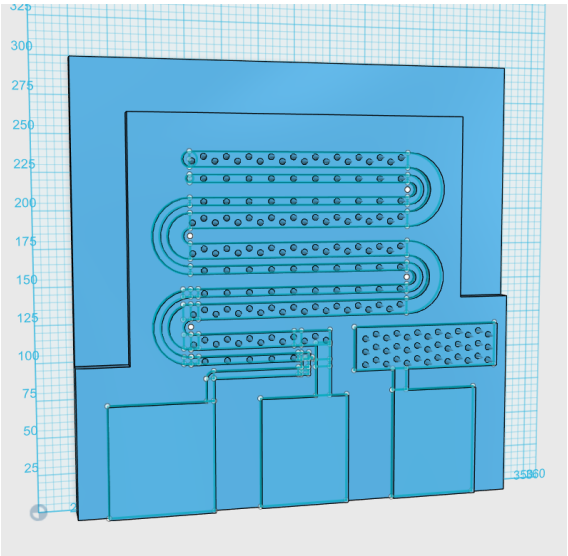

Figure 10: Schematic of the non-reusable sensing chip with microneedles and electrode layout.

7.4 Hardware

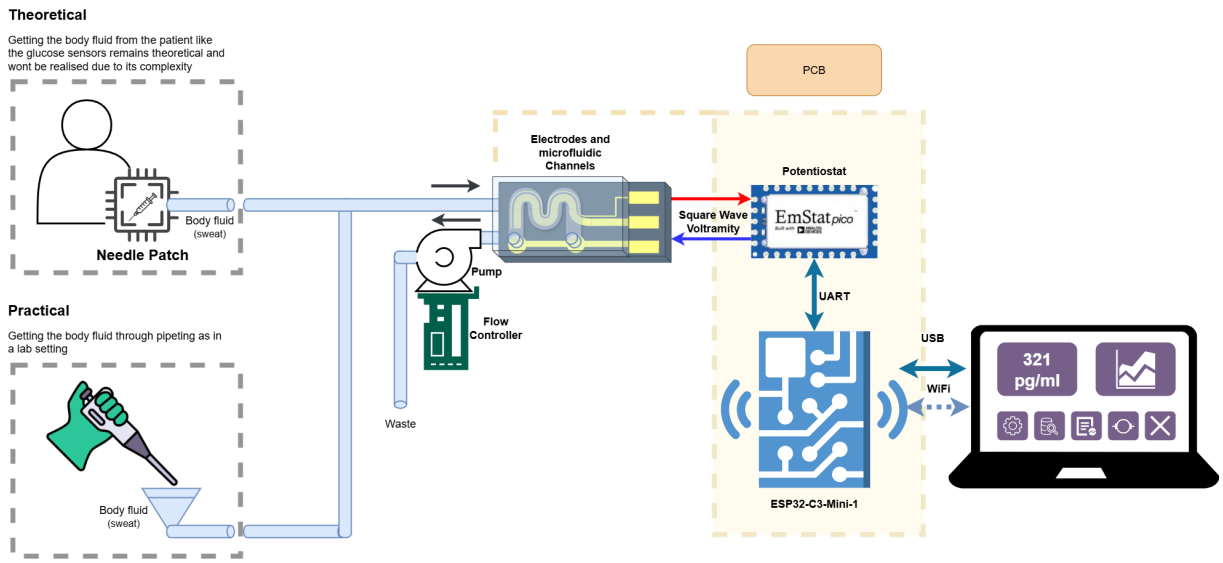

Figure 11: Overall schematic of the working system

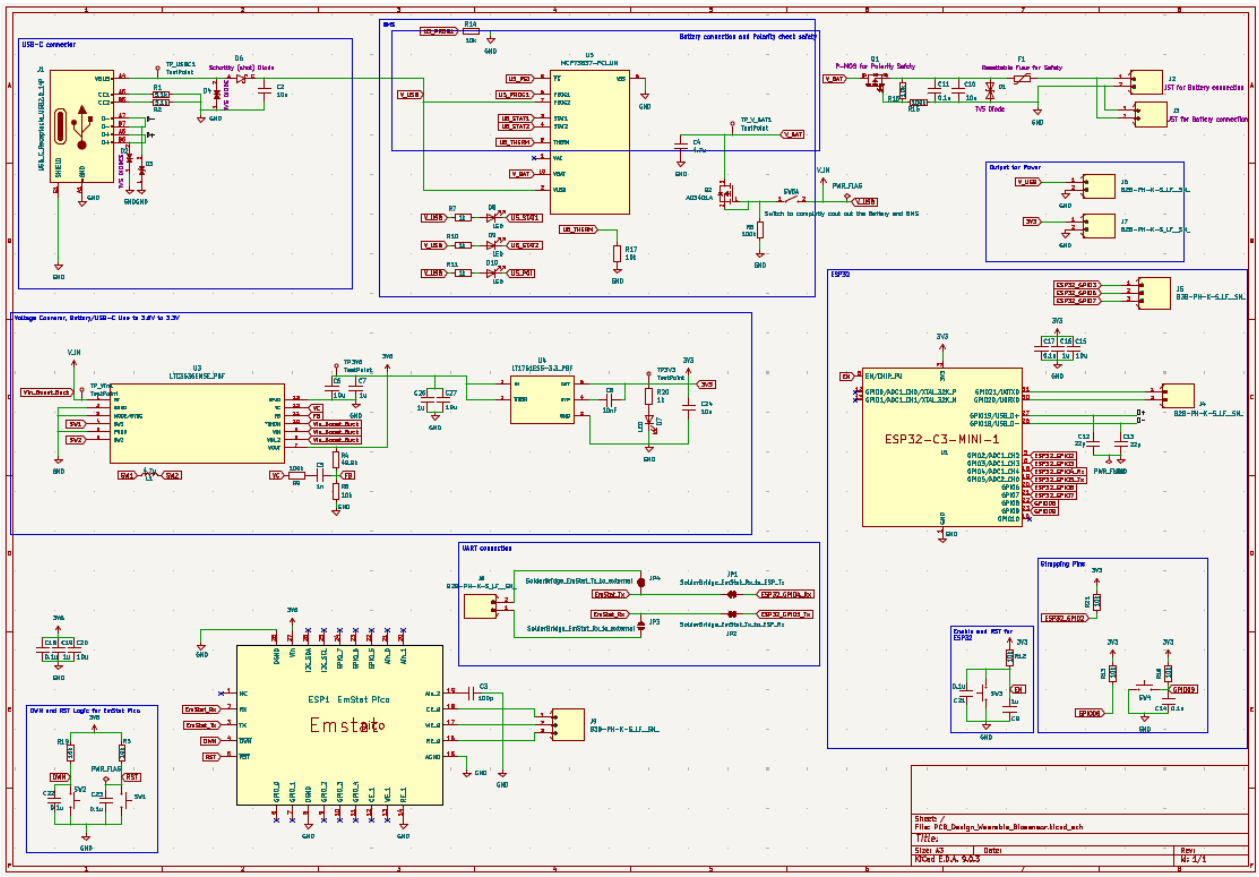

Figure 12: PCB schematics, developed with KiCad

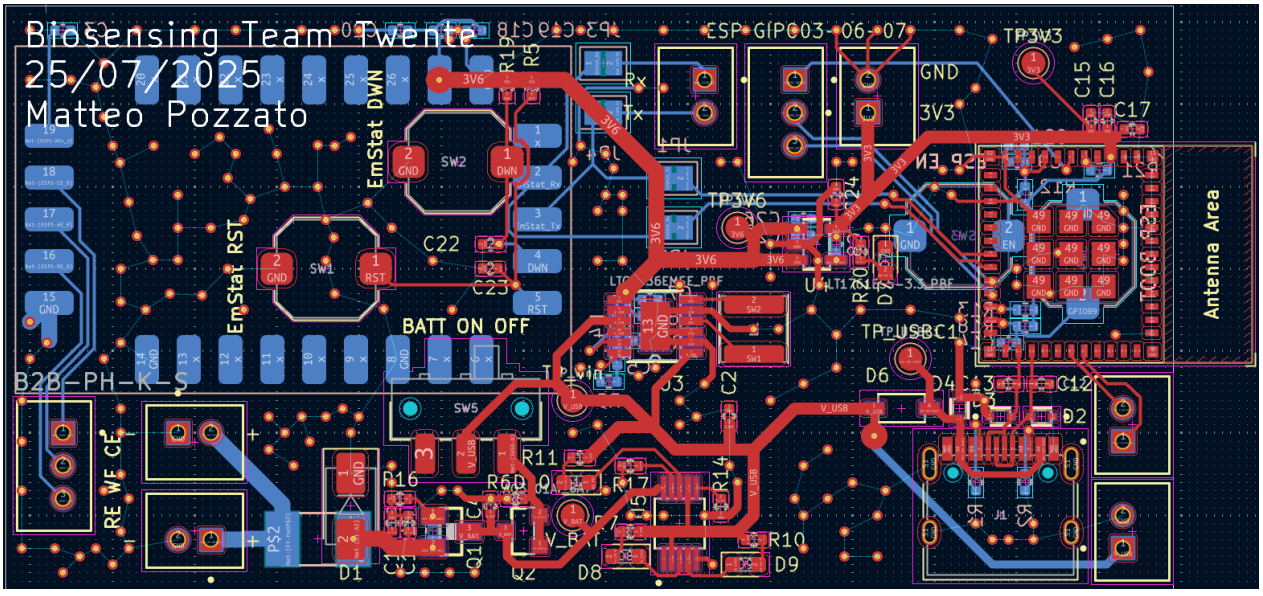

Figure 13: PCB layout, developed with KiCad

7.5 Wearable sensor design concepts

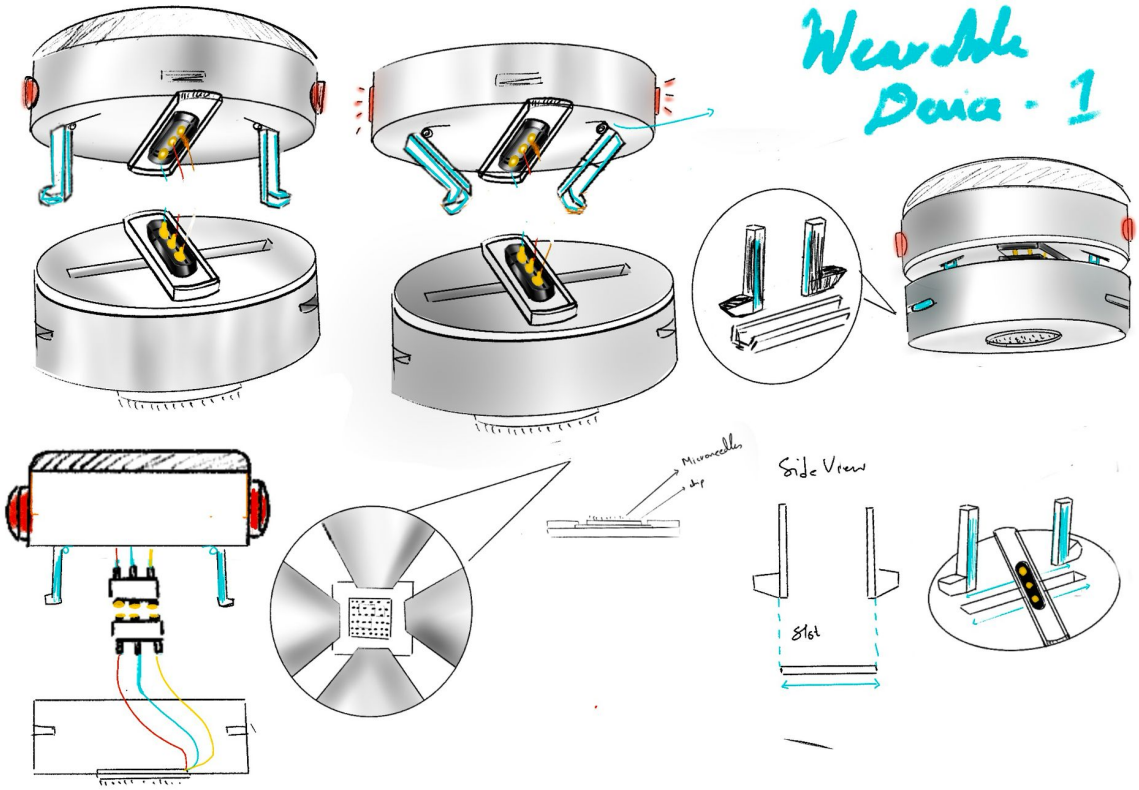

Figure 14: Wearable device concept 1

The first concept is a wearable biosensor with angled clamp arms secured by a spring mechanism similar to a clothing clip, enabling quick attachment and detachment.

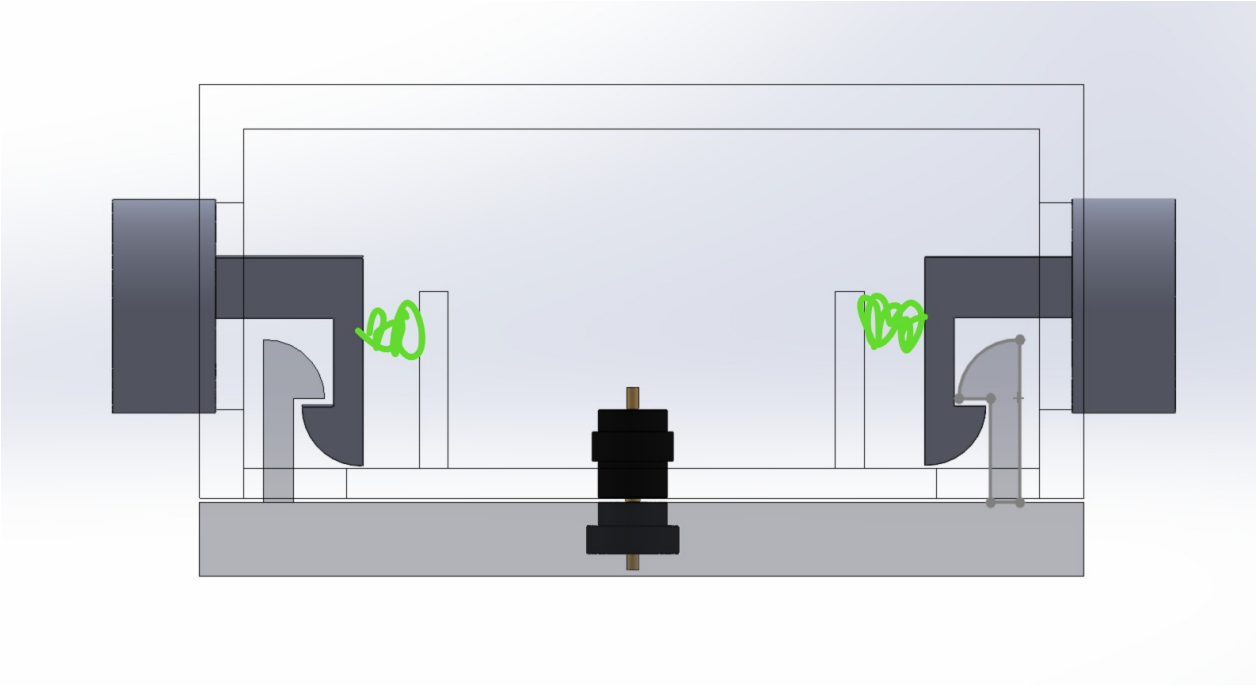

Figure 15: Wearable device concept 2

The second concept uses a comparable spring-loaded clamp design, where compression springs push the arms outward until they are pressed inward to release the lock.

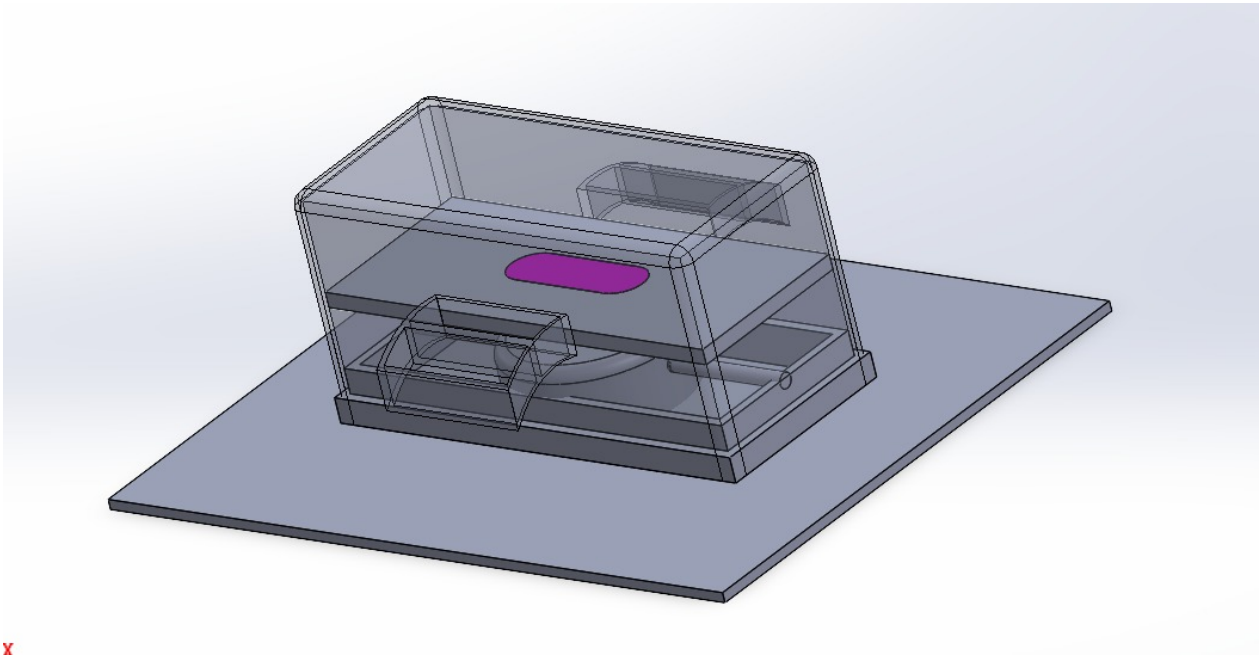

Figure 16: Wearable device concept 2

This concept uses two buttons on both sides and spring to lock the module in place. To detatch the two modules, the upper module will be turned clockwise.

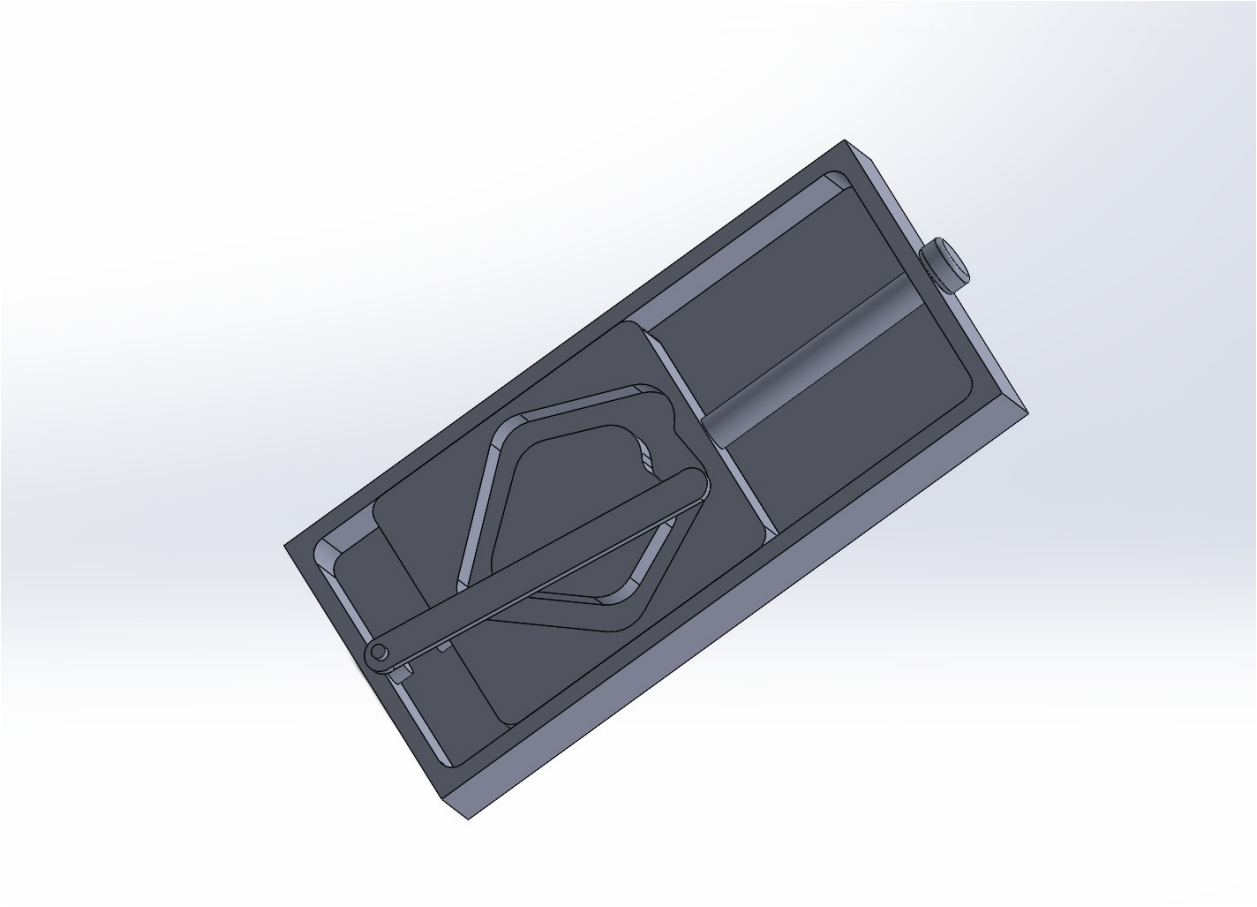

Figure 17: Wearable device concept 2

This concept showcases our attempt to include a press to open and another press to close mechanism to attach and detatch the two modules.

7.6 Wearable sensor design 3D models

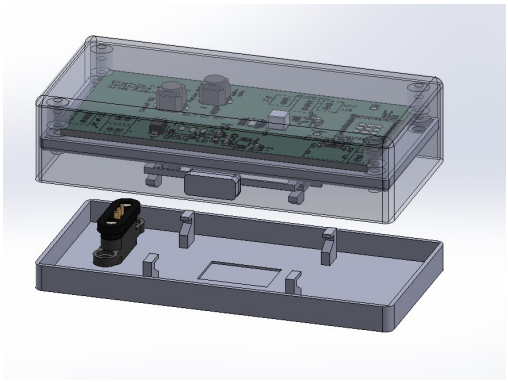

0.45
(a) b

Figure 18: Top view

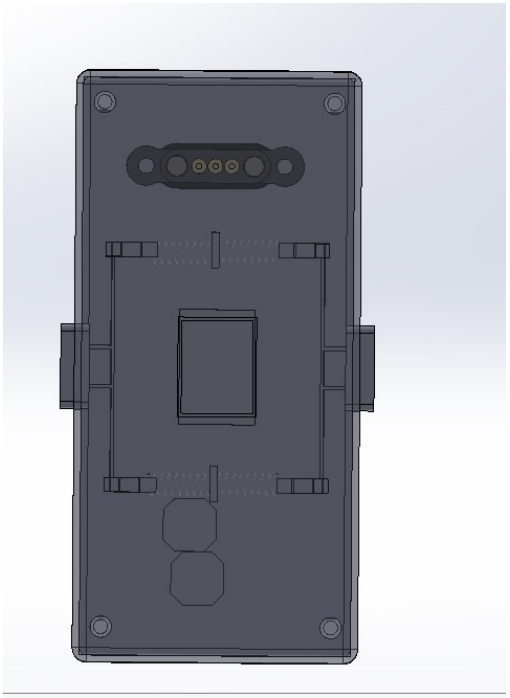

0.45
(a) b

Figure 19: Bottom view

Figure 20: First iteration of wearable device

7.7 Material Requirements for wearable biosensor

7.7.1 Conditions of Use

To determine the appropriate material for the device, we first analyzed the **conditions of use** to understand the environmental, mechanical, and safety demands the material must meet. This informed the selection criteria listed below.

Location:
Hospital environment — cardiac surgery ward, ICU, high-dependency unit (HDU), recovery ward.

Duration and Use:
Worn continuously for 48 hours, including during sleep. Device must remain functional during patient movement, repositioning, and rest.

Patient-Related Incidents:

- **Exposure** to wet hands, bodily fluids (blood, urine, sweat).
- **Spillage** of water or disinfectant.
- **Potential impact** from sitting or lying on the device.
- **Dropping** the device on the floor.
- **Slippage** off the body (requires grippy or ergonomic surface texture).

Use-Related Incidents (Electronics):

- Risk of **localized heating** from internal components (sensors, battery, wireless transmission).
- Must remain **thermally stable and non-conductive** externally to ensure patient safety.

Conditions of Storage (Before Use):

- Devices typically stored in **clean, dry, temperature-controlled** cabinets or supply rooms (15–25°C, low humidity).
- Packaging may be **sterile or clean**, depending on patient-contact requirements.

7.7.2 Required Properties of the Material

Mechanical:

- **High impact resistance** (for drops or compressive forces if sat on).
- **Durable under continuous wear** and bending.
- **Minimum yield strength** to prevent cracking or deformation during handling or use.
- **Good dimensional stability** to protect internal electronics.

Thermal:

- **Withstand moderate temperature increases** without softening or releasing fumes.
- **Low thermal conductivity** to protect skin from internal heating.
- **Tolerant to hospital-grade disinfectants** (wipes, alcohol-based cleaners).

Costs:

- **Low-to-moderate cost** per unit to allow disposability or affordable re-use.
- Must be **economical for mass production** in injection molding.

Flexibility:

- Should offer **some flexibility or resilience** without brittleness.
- Preferably **semi-rigid casing with grippy surface**.

Aesthetics:

- **Neutral, medical color palette** (e.g., white, grey, light blue).
- **Smooth and cleanable surface**, ergonomic and unobtrusive design.
- **No sharp edges or uncomfortable surfaces**.
- **Not exceed 10 × 10 cm** for the part that contacts the skin.

Sterilization:

- Ideally a **cleaned but non-sterile** device (not invasive).

Sustainability:

- **Recyclable thermoplastic** preferred.
- If disposable: evaluate **eco-friendly plastics** or biodegradable alternatives.

Biocompatibility:

- Compliant with **ISO 10993 standards** for skin contact (*Biological evaluation of medical devices – Part 23: Tests for irritation*, 2021).
- **Non-irritant, hypoallergenic**, and safe for sweaty or sensitive skin.

7.8 Customer interviews

Name	Position	Contribution	Location
Jeroen Vollenbroek	Researcher, Artificial Kidney	Use case	UMC Utrecth
Joos Hoenderop	Physiologist	–	–
Jasper Boomker	Dutch Kidney Foundation	–	–
Dick Thijssen	CardiacCare@Home Project	–	–
Martin Bennink	Professor, Applied Nanotechnology	–	–
Hans Krabbe	Researcher, AKI-Sepsis	Use case	MST
Tamar van der Aart	PhD, AKI-Sepsis	Use case	Radboud
Wytze Vermeijden	Intensivist	–	MST
Peter Oosterhoff	MedTech Quality Assurance & Regulatory Affairs Expert	Clinical validation & regulations	TechMed
Tugrul	Researcher and professor	Clinical validation & regulations	University of Twente and UMC Utrecht
Marcel Zevenbergen	Tech lead biochemical sensors	Use case	IMEC
Sandy Grishaverr-Kalisingh	Member, Supervisory Board of Dutch Kidney Foundation; Sr. Program Officer at NWO	Support in stakeholder engagement	Nierstichting / NWO
Wytze Vermeijden	Cardiothoracic surgeon	Clinical pathway and protocol	MST
Fokko Pieter Wieringa	PhD, Principal Scientist at IMEC and professor		IMEC, UMC Utrecth
Sanne Borremans	Nurse Practitioner Dialysis & Nephrology	Clinical vlaidation	Bravis ziekenhuis

Table 5: Experts consulted and their contributions.

Table 6 below shows the risk description and incidence defined from the interviews with the stakeholders, to come up with design requirements for the device.

Hazard	Description	O	S	D	RPN
Detachability	Patch may detach from skin due to sweating or movement.	4	6	8	192
Alarm missed	Nurse fails to hear the alarm after creatinine rise, delaying intervention, hence the device is useless.	6	10	9	540
Spillage onto device	Liquid is spilled onto the device.	9	2	1	18
Overheating	Electronics may overheat during use, causing discomfort or burns.	2	8	6	96
Biological and chemical hazards	Microneedles may be contaminated by bacteria, fungi, toxins, etc., during handling or application.	4	7	5	140
Material Allergy	Patient may react to microneedle or adhesive materials (e.g., rash).	3	6	5	90
Data Transfer	Wireless transmission to EHR may fail or be delayed.	5	7	5	175
Device Malfunction	Internal component failure (e.g., sensor, battery) halts operation.	4	9	8	288
Inadequate Packaging	Improper packaging leads to device degradation or contamination pre-use.	3	9	5	135
Ambiguous Instructions	Instructions on the kit are unclear to nurses due to language barriers or other reasons.	2	6	1	12
Reuse of single-use component	Single-use microneedles are reused on another patient.	3	8	8	192
Running out of Battery	Device battery is depleted.	2	1	1	2
Specificity (False Positives)	Alarm is triggered when no actual danger is present.	5	2	8	80
Sensitivity (False Negatives)	Alarm is not triggered even though the patient is in danger.	6	9	8	432

Table 6: Hazard traceability matrix with color-coded (values form 1-10) Occurrence (O), Severity (S), and Detection (D) levels, based on defined risk ranges.

7.9 Patient Journey

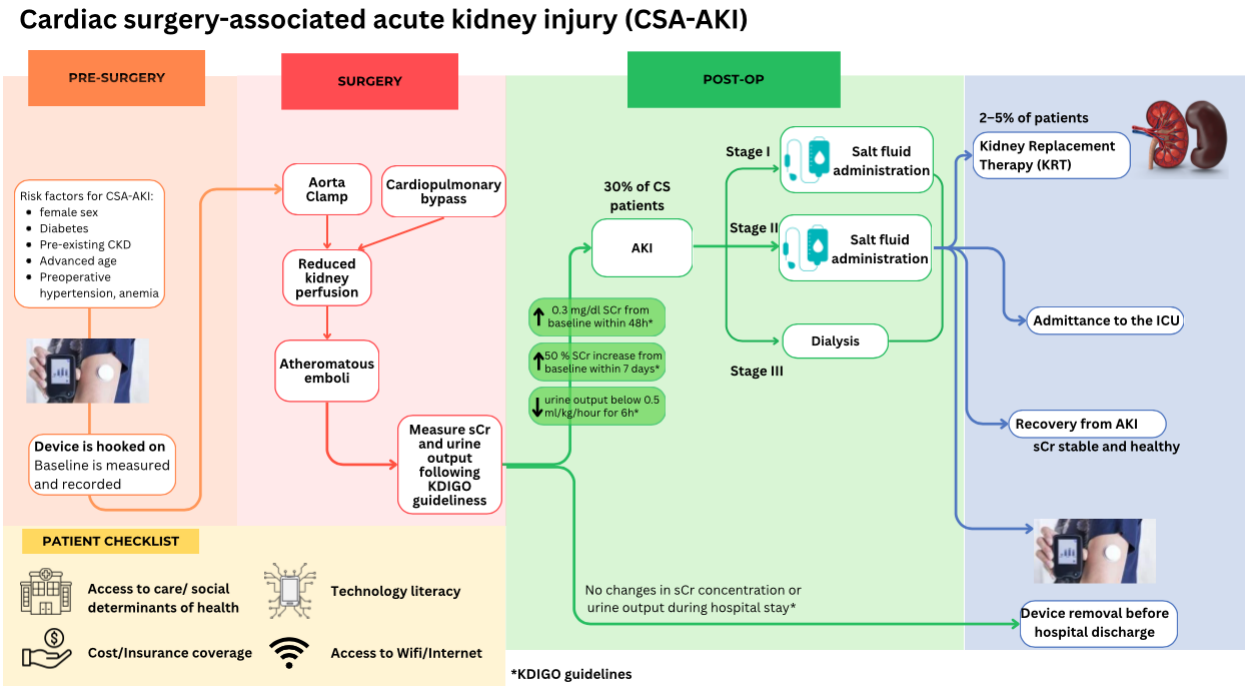

Figure 21: Patient Journey derived from interviews.

7.10 Clinical validation sample size calculation

A multicentre prospective cohort study to evaluate the usability and integration of a wearable biosensor in cardiac surgery patients and nursing staff, and its effectiveness in enabling earlier detection of AKI, in comparison with standard blood-based diagnostic methods.

The sample size formula for a cohort study is the following:

$$n = \frac{(Z_{\frac{\alpha}{2}} + Z_{\beta})^2 \cdot 2 \cdot \sigma^2}{d^2}$$

Where:

- n = sample size per group
- σ^2 = Variance of the outcome (sqrt of the standard deviation)
- $Z_{\frac{\alpha}{2}}$ = Z-score for the significance level
- Z_{β} = Z-score for the power
- d = Clinically significant difference/effect size

We expect the biosensor to detect AKI ≈ 6 hours earlier than serum creatinine. Hence we can determine a clinically significant difference of $d \approx 6$ hours, with a standard deviation of $\sigma = 8$ hours. Since 5% is a standard threshold to minimize the risk of a false positive error, we get α

(two-tailed) = 0.05, $Z_{\frac{\alpha}{2}}$ = 1.96. A high probability of detecting the study's true effect is expected, hence an 80% of probability is chosen (Beaubien-Souligny et al., 2018).

After substituting the values in the equation, the calculated sample size is 28 patients. However, according to (Vives et al., 2019) only 30% of the cardiac patients included in the study are expected to develop AKI. Hence, 28 patients are needed to power the test, but in total $\frac{28}{0.30} \approx 94$ patients are needed to ensure a robust sample size to detect a clinically significant difference.

7.11 Inclusion and Exclusion Criteria

Patient Group:

- **Inclusion Criteria:** Patients scheduled for cardiac surgeries will receive an information letter during pre-admission consultation and will be asked for informed consent during admission.
- **Exclusion Criteria:**Participants shall be excluded if they are mentally incapable of providing informed consent or if the nature of their injury prevents them from wearing the sensors. Patients with known allergies to adhesive materials used in the sensor patch or those participating in other clinical trials that could interfere with this study will be excluded.

Practitioner Group:

- **Inclusion Criteria:**Practitioners currently employed at one of the three participating hospitals.
- **Exclusion Criteria:**Practitioners with less than 2 years of experience in their current role or those not directly involved in the care of cardiac surgery patients will be excluded.

This approach ensures that both the clinical performance and the practical usability of the device are validated in diverse clinical settings, supporting broader applicability and regulatory readiness.

7.12 Data Handling Procedures

This study will adhere to strict protocols for data handling to ensure the privacy and security of participant information. The following procedures will be implemented:

1. **Informed Consent:** All participants will receive detailed information about the study and will be required to provide written informed consent before any data is collected, in accordance with the Declaration of Helsinki (World Medical Association, n.d.).
2. **Data Collection:** using secure and encrypted methods to ensure confidentiality. Each participant will be assigned a unique identifier to pseudonymize the data and protect their identity, following guidelines for the appropriate use of personal data in scientific research according to the GDPR (European Medicines Agency, 2023) .

3. **Data Storage:** on secure servers with restricted access to authorized personnel only. Data will be stored in compliance with GDPR guidelines to ensure the protection of personal information (European Medicines Agency, 2023).
4. **Data Processing:** will be conducted using secure and validated software tools. Access to data will be limited to authorized researchers and will be monitored to prevent unauthorized access.
5. **Data sharing** in accordance with GDPR guidelines and will be limited to authorized parties only. Any data shared will be pseudonymized to protect participant identities (European Medicines Agency, 2023).

By following these procedures, we aim to ensure the integrity and confidentiality of the data collected in this study, in compliance with ethical standards and regulatory requirements.

7.13 Data Collection

Definitions and Diagnostic Metrics The following metrics will be calculated using the standard binary classification framework, based on matched biosensor alerts and serum creatinine results:

- **True Positive (TP)**: Alarm sounds, and AKI is confirmed by reference blood test.
- **False Positive (FP)**: Alarm sounds, but AKI is not confirmed by reference test.
- **False Negative (FN)**: No alarm, but AKI is detected during routine morning draw.
- **True Negative (TN)**: No alarm, and no AKI is present.

The diagnostic performance metrics are then calculated as:

$$\text{Sensitivity} = \frac{TP}{TP + FN} \qquad \text{Specificity} = \frac{TN}{TN + FP}$$

$$\text{Positive Predictive Value (PPV)} = \frac{TP}{TP + FP} \qquad \text{Negative Predictive Value (NPV)} = \frac{TN}{TN + FN}$$

-Accuracy (Quantitative Evaluation) This component focuses on validating the analytical accuracy of the biosensor in measuring creatinine levels compared to the hospital's standard blood-based laboratory method.

Protocol:

- At each routine blood draw (every 24 hours), a simultaneous reading will be recorded from the biosensor.
- This ensures the collection of matched data points across the patient's hospital stay.

Statistical Analyses:

- Pearson correlation coefficient (r) to assess linear correlation
- Mean Absolute Error (MAE) and Root Mean Squared Error (RMSE) for deviation measurement

- Bland-Altman plots for agreement analysis

These measures will assess both point accuracy and the biosensor's ability to track creatinine trends over time.

-Usability (Qualitative Evaluation) Usability evaluation will capture the perspectives of patients, nurses, and physicians regarding the biosensor's integration into clinical workflows, comfort, and overall acceptability.

Participants:

- **Patients** wearing the device
- **Nurses** involved in its application, monitoring, and data collection
- **Physicians** responsible for clinical decision-making based on biosensor outputs

Timing:

- **Pre-operative:** Initial impressions and expectations
- **Post-operative:** Feedback on integration into care routines, interference, and comfort
- **Post-discharge:** Overall experience and retrospective evaluation

Data Collection Methods:

- Semi-structured interviews conducted at each stage
- Structured surveys using Likert scales and open-ended questions

Analysis:

- Interview transcripts will be thematically analyzed.
- Survey responses will be summarized using descriptive statistics and qualitative synthesis.

-Value Validation (Quantitative Modeling) This component models the clinical and economic value of earlier AKI detection using biosensor-derived ΔT.

7.13.1 Handling of Missing or Noisy Data

- Gaps > 1 hour in biosensor data will be flagged and excluded from sensitivity/specificity analysis.
- Delayed lab draws (> 1 hour post-alarm) are excluded from time-to-detection analysis but retained for classification.
- Patients with $> 20\%$ missing sensor data will be excluded from primary analysis.

To validate device accuracy beyond alarms, paired sensor and lab values will be compared using:

- Bland-Altman analysis (bias and agreement)
- Pearson correlation coefficient (r)

- Root Mean Squared Error (RMSE)

7.14 Expected Performance Metrics

To estimate the diagnostic yield during the Validation study, we assume:

- **AKI prevalence** in the target population: 20%
- **Study population size**: $N = 94$ patients
- **Target sensitivity**: 90%
- **Target specificity**: 90%

From these values, we can estimate the expected distribution of outcomes:

- True AKI cases $= N \times 0.20 = 18.8 \approx 19$
- Non-AKI cases $= N \times 0.80 = 75.2 \approx 75$

Using the formulas:

$$\begin{aligned}
\text{TP} &= \text{Sensitivity} \times \text{AKI cases} = 0.9 \times 19 = 17.1 \approx 17 \\
\text{FN} &= \text{AKI cases} - \text{TP} = 19 - 17 = 2 \\
\text{TN} &= \text{Specificity} \times \text{Non-AKI cases} = 0.9 \times 75 = 67.5 \approx 68 \\
\text{FP} &= \text{Non-AKI cases} - \text{TN} = 75 - 68 = 7
\end{aligned}$$

Expected Performance Metrics:

$$\begin{aligned}
\text{PPV} &= \frac{TP}{TP + FP} = \frac{17}{17 + 7} \approx 70.8\% \\
\text{NPV} &= \frac{TN}{TN + FN} = \frac{68}{68 + 2} \approx 97.1\%
\end{aligned}$$

Implication: These estimates indicate that, under the given assumptions, the biosensor would produce relatively few false positives or false negatives, and yield high negative predictive value (NPV). The positive predictive value (PPV), while slightly below the 75% target, may still be clinically acceptable given the early detection benefit and safety profile. These figures are used for feasibility assessment and refining power calculations.

7.15 Performance Requirements for Clinical Viability

Performance Thresholds To be considered clinically viable, the biosensor must meet or exceed the following thresholds:

- Sensitivity $\geq 90\%$
- Specificity $\geq 90\%$

- Positive Predictive Value (PPV) $\geq$ 75%
- Negative Predictive Value (NPV) $\geq$ 95%

Justification from Literature These thresholds are derived from best practices in AKI biomarker development and early warning systems for critical care:

- High sensitivity is crucial for early AKI detection, as delayed diagnosis increases mortality and risk of requiring renal replacement therapy (RRT). The KDIGO guidelines and biomarker validation studies recommend sensitivity $\geq$90% in high-risk clinical environments (Kellum et al., 2015; Kashani et al., 2013).
- Specificity $\geq$90% is needed to reduce false alarms and alarm fatigue, which can erode clinician trust in device outputs (Koyner, Carey, Edelson, & Churpek, 2018).
- High NPV ($\geq$95%) ensures that the device can confidently rule out AKI, especially important in intermediate-risk patients where overtreatment is costly and unnecessary (Chawla, Eggers, Star, & Kimmel, 2014).
- PPV of at least 75% supports efficient clinical triage and response, ensuring that a majority of alarms correspond to actionable cases.

7.16 Competitor Products

The table below shows a comparison of current products available in the market for the detection and/or monitoring of creatinine levels.

Name and Company	Target patients	Technology	Description	Output	Measurement range	FDA Approval	Monetary Valuation
StatSensor (Nova Biomedical, n.d.)	General	Single-use biosensor	Whole blood creatinine testing	Creatinine and eGFR results in 30 seconds	Creatinine: 0.3–12.0 mg/dL (27–1056 µmol/L)	-	Not available
i-STAT Creatinine test (Abbott Point of Care, n.d.)	General	Point-of-care biosensor	Rapid creatinine testing	Results in 2 minutes	Sample size: 65 µL; Creatinine: 0.2–20.0 mg/dL (18–1768 µmol/L)	FDA approved	Not available
Transdermal GFR System (Medibeacon, n.d.)	General	Transdermal fluorescence	Injectable exogenous fluorescent tracer for GFR assessment; no blood or urine samples required; not intended to diagnose AKI	GFR measurement	Not applicable	FDA approval expected Jan 2025	Not available
Clarity RMS (RenalSense) (Chalice Medical, 2023)	ICU Patients	Urine flow monitoring	Real-time urine flow measurement replacing urometer; data sent to hospital systems	Urine flow rate	Not applicable	CE-marked class 2a	Console: £3,810 (5–10 years lifespan); Disposable sensor kit: £65 per person; Standard urometer cost: £8–£10 per person

Table 7: Comparison of current devices targeting kidney function monitoring.

7.17 Experimental Validation

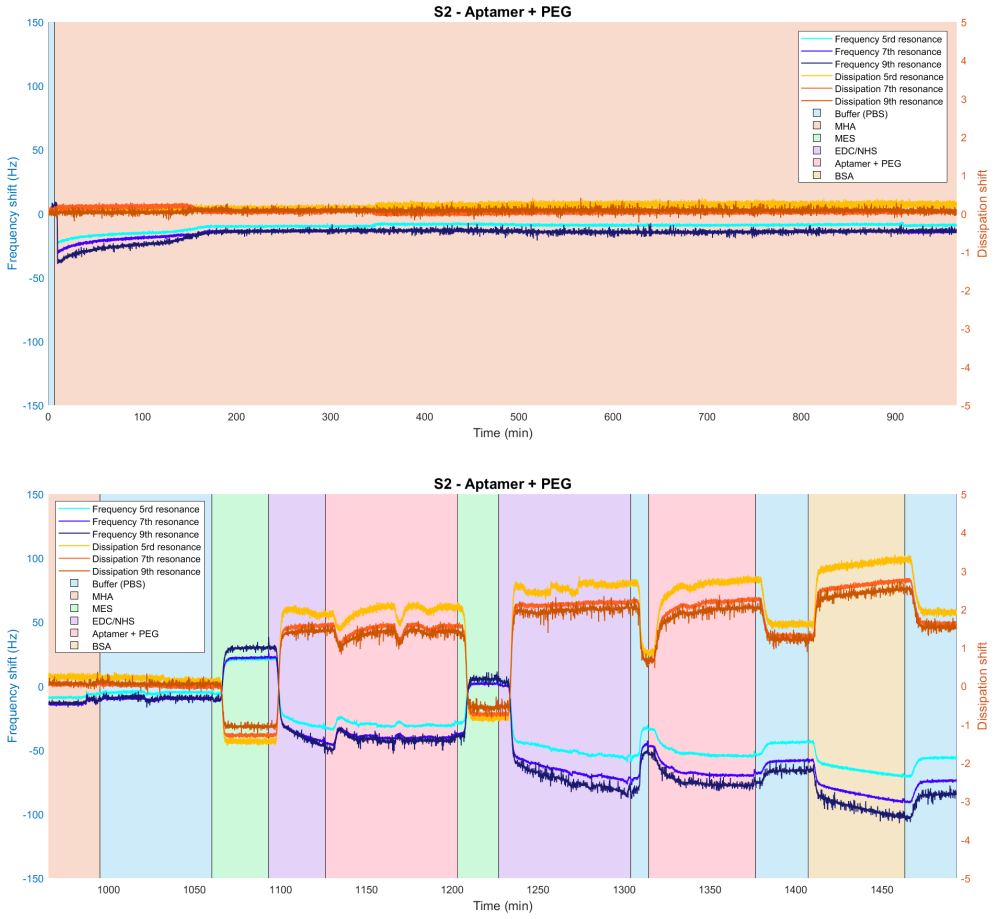

Figure 22: results for the functionalization of the chip. The top image shows the formation of an MHA SAM overnight, and the bottom image shows the / activation, the binding of the aptamer and PEG to the MHA monolayer, and an antifouling test with bovine serum albumin (). The activation and binding of aptamer and PEG steps were repeated due to an initial low coverage.

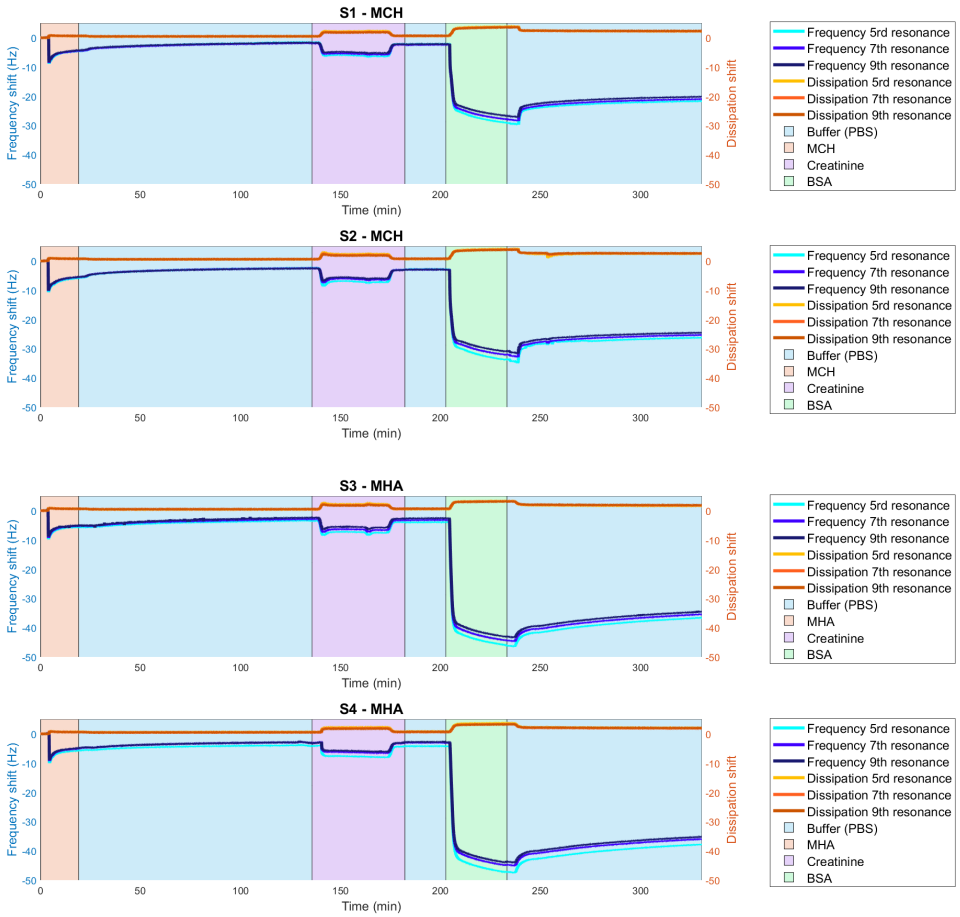

Figure 23: results for an MCH (top) and MHA (bottom) formation, followed by an antifouling test with .

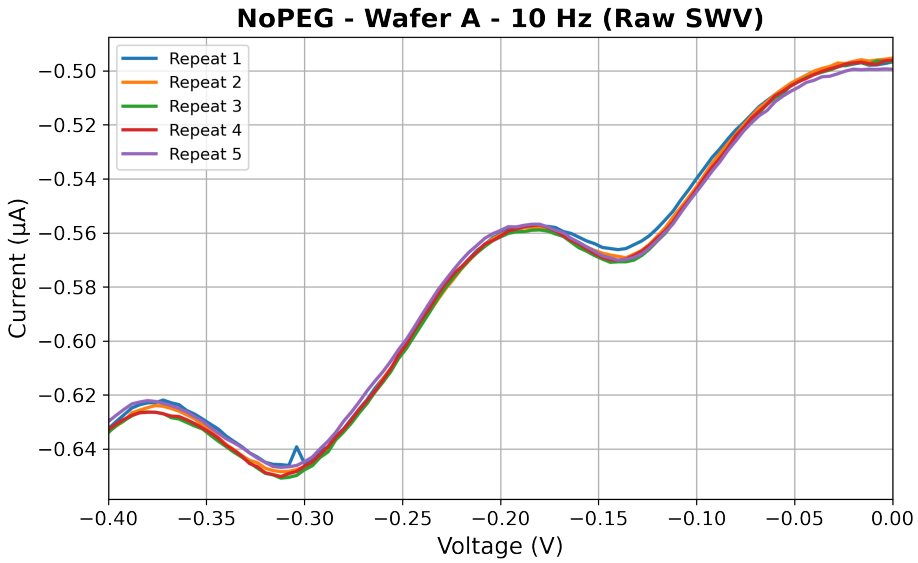

Figure 24: SWV for the functionalized surface without PEG. Multiple repeats for the same experiment are shown. The peak below -0.30 V is attributed to the methylene blue reporter redox signal (Mahlum et al., 2021).

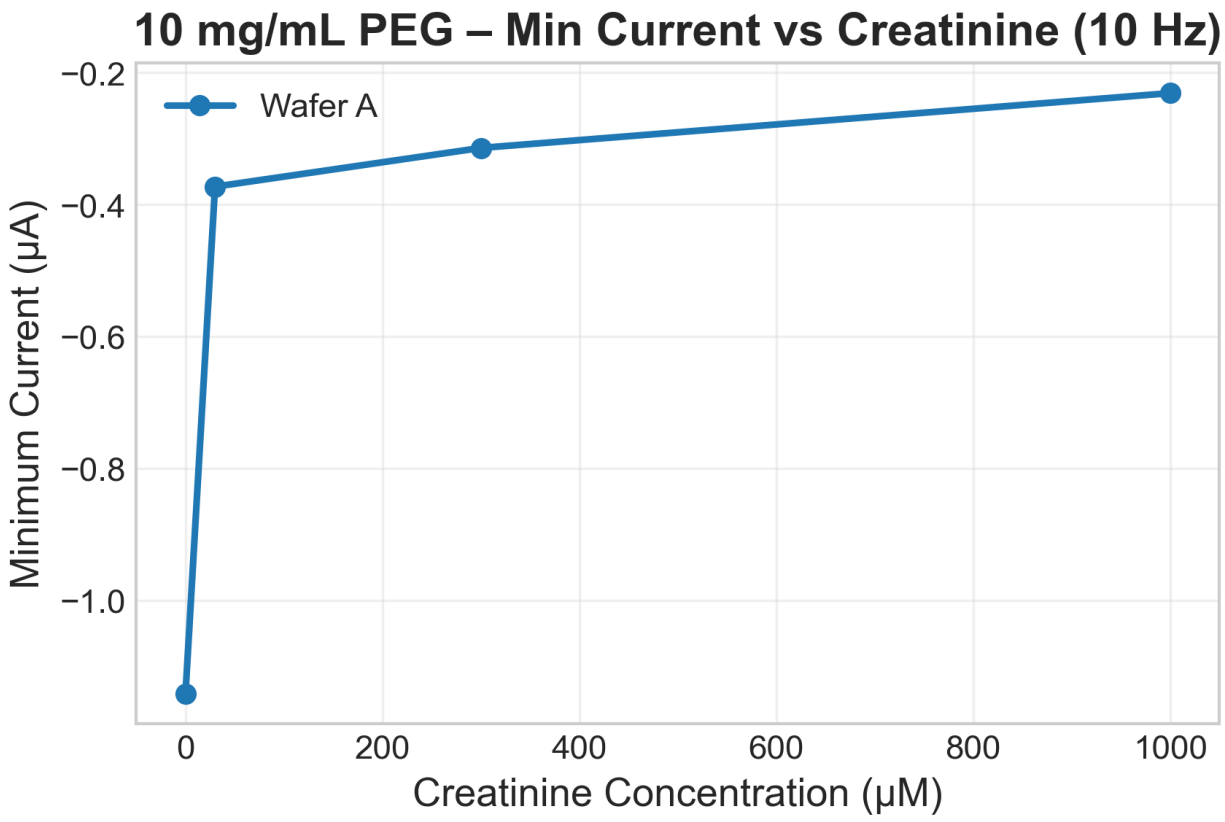

Figure 25: Plot for peak current vs. creatinine concentration for the wafer functionalized with 10 mg/mL PEG concentration (Figure 6, top). The results cannot be taken fully quantitatively since the measurement procedure did not carefully control for exposed surface area and due to limited data points, but a general qualitative trend can be observed.